Physics in Medicine & Biology

IPEM Institute of Physics and Engineering in Medicine

TOPICAL REVIEW • OPEN ACCESS

Photoacoustic imaging for guidance of interventions in cardiovascular medicine

To cite this article: Sophinese Iskander-Rizk *et al* 2019 *Phys. Med. Biol.* **64** 16TR01

IOP Publishing Phys. Med. Biol. 64 (2019) 16TR01 (19pp) https://doi.org/10.1088/1361-6560/ab1ede

Physics in Medicine & Biology

IPEM Institute of Physics and Engineering in Medicine

OPEN ACCESS

TOPICAL REVIEW

Photoacoustic imaging for guidance of interventions in cardiovascular medicine

Sophinese Iskander-Rizk[1], **Antonius F W van der Steen**[1,2] **and Gijs van Soest**[1,3]

[1] Department of Cardiology, Biomedical Engineering, Erasmus MC University Medical Center Rotterdam, Wytemaweg 80, 3015 CN Rotterdam, The Netherlands

[2] Faculty of Applied Sciences, Department of Imaging Physics, Delft University of Technology, Lorentzweg 1, 2628CJ Delft, The Netherlands

[3] Author to whom any correspondence should be addressed.

E-mail: g.vansoest@erasmusmc.nl

Keywords: photoacoustic, cardiovascular medicine, intervention guidance, review, athersoclerosis, ablation, arrhythmia

RECEIVED
11 February 2019

REVISED
4 April 2019

ACCEPTED FOR PUBLICATION
2 May 2019

PUBLISHED
21 August 2019

Abstract

Imaging guidance is paramount to procedural success in minimally invasive interventions. Catheter-based therapies are the standard of care in the treatment of many cardiac disorders, including coronary artery disease, structural heart disease and electrophysiological conditions. Many of these diseases are caused by, or effect, a change in vasculature or cardiac tissue composition, which can potentially be detected by photoacoustic imaging. This review summarizes the state of the art in photoacoustic imaging approaches that have been proposed for intervention guidance in cardiovascular care. All of these techniques are currently in the preclinical phase. We will conclude with an outlook towards clinical applications.

1. Introduction

Cardiovascular disease (CVD) remains the number one cause of death worldwide, killing 17.7 million people in 2015 (WHO 2015). Major risk factors are lifestyle-related: smoking, obesity, diet, and lack of exercise are major determinants for the occurrence of all cardiac and vascular conditions. While most of these factors are modifiable in principle, strategies to alter unhealthy behaviour have had limited success so far.

Incidence of cardiovascular disease is progressive with age. Improved conditions, greater access to sanitation, medication and health care, and overall reduction of poverty have led to a global increase in life expectancy. This development, which overall is excellent news for public health, comes with the widespread adoption of a Western diet and lifestyle which are associated with increased cardiovascular risk. Today, more than 80% of CVD deaths occur in low- and middle-income countries (Abubakar *et al* 2015). Increased life expectancy is associated to a higher incidence of heart failure. This association could be explained by a heightened probability of damage to the heart caused by a survived myocardial infarction (MI; a heart attack), for instance, or poorly treated rhythm disorders. Providing adequate and affordable care to patients with CVD worldwide is a major challenge in the coming decades.

Treating all these patients with cardiac disease will depend strongly on technology; more specifically on the development of devices for minimally invasive treatment and for imaging guidance of these interventions. In minimally invasive interventions, functional catheters are advanced to the heart of the patient through a small incision in an artery or vein, to locally treat the condition. Catheter-based treatment strategies have a huge benefit for patients and the healthcare system as a whole. Our ageing population will develop an epidemic of CVD, which requires adequate treatment to maintain quality of life and prevent progression of the disease. The alternative to minimally invasive treatment in the heart is cardiac surgery. Surgery requires opening the sternum, and while this has become a routine operation, the intervention requires hospitalization for at least a week and full recovery takes about a year, including 2–3 months of inability to work. In contrast, catheter-based treatments can frequently be done without requiring an overnight stay: patients are admitted in the morning and discharged in the evening of the same day provided there were no complications. Recovery takes days rather than months, and the patient experiences much less physical trauma than in the case of an open surgery. The advantages of minimally

invasive interventions in cost, demands on the healthcare system, and lost productivity are vast, compared to surgery.

In minimally invasive treatment, interventionists have no direct line-of-sight to neither the instruments in use to treat the patient, nor to the pathology being treated. In today's practice, the most common image guidance tool is x-ray fluoroscopy or angiography. It provides a 2D projection image of the heart and vessels, which are moving organs in three dimensions. Visualization of interventional catheters is frequently poor, depending on the presence of radiopaque markers on the devices. Soft tissues hardly present any image contrast and vessels are visualized by injection of a contrast dye (angiography), which delineates the lumen but not the artery wall (Mintz and Guagliumi 2017). Moreover, the cavities of the heart can also not be effectively visualized by means of x-ray contrast. Thus, in order to meet the efficacy and safety outcomes of surgical treatment, it is crucial for the interventionist to access real-time, accurate imaging that provides functional image contrast at an adequate resolution. A real-time imaging modality is paramount to (1) support instrument navigation towards the treatment site, to (2) inform the therapeutic strategy, to (3) monitor the progress of the intervention and to (4) check its result. Photoacoustic (PA) imaging is unique in combining speed, compact instrumentation, and innate tissue type contrast (by optical absorption). These features lend it significant potential for interventional imaging in cardiology.

1.1. Scope of this review

This review discusses the current state of the art in PA imaging for cardiovascular applications, specifically focusing on techniques that aim at guidance of cardiac and vascular interventions. PA imaging is a hybrid imaging modality, merging advantages of optical and ultrasonic imaging. Optical absorption can provide chemically specific information, for instance on the oxygen saturation of blood. Purely optical imaging methods, however, require a coherent wavefront, which is poorly preserved due to tissue scattering, limiting the imaging depth. Photoacoustics, on the other hand, relies on both optical power and coherence of resulting acoustic waves for imaging, and thus allows one to image chemical information relatively deep (up to several centimetres) in biological structures. Deeper targets may be reached by miniaturization into endoscopic probes.

The term 'photoacoustic' was introduced in cardiovascular medicine in the context of laser tissue ablation, for instance in decalcification of aortic valve leaflets (Williamson *et al* 1993) or coronary laser angioplasty and clot removal (Quan and Hodgson 1996, Topaz *et al* 1996, 1998). It was used to indicate the photomechanical effects of cavitation bubble formation and the subsequent shockwave that caused tissue damage (Isner *et al* 1992, van Leeuwen *et al* 1992, 1993). The acoustic signature of these violent events created by high-energy ultraviolet (excimer) or mid-infrared pulse absorption only had an intended therapeutic use. The usage of the word 'photoacoustic' has evolved to imply non-destructive applications such as imaging, sensing or tissue characterization, rather than an ablation mechanism. In this review, we will discuss photoacoustics as an interventional imaging tool, not as a therapeutic intervention on its own.

CVD comprises interrelated and frequently interacting conditions such as vascular disorders, rhythm disorders, structural heart disease, and microvascular disease. As a result, conditions may be multifactorial from a clinical standpoint, with sometimes unclear boundaries. In an actual patient, the location of a previous MI may become a nidus for electrical conduction disorders that result in arrhythmias (Roes *et al* 2009). Atrial fibrillation, one such arrhythmia, can cause circulating thrombi, which can lodge themselves in the vasculature of the brain, causing an ischemic stroke (Wolf *et al* 1978). The uniquely tissue-specific image contrast of photoacoustics may, one day, help in unravelling the intricate web of causes and effects in CVD. This review is organized according to the various single-diagnostic applications for which PA imaging technologies have been developed. We summarize the advances in PA research for cardiovascular interventions, also outlining today's practical procedures where PA image guidance may fulfil an unmet need. We discuss image contrast mechanisms, proposed innovative devices, and their envisioned roles in cardiovascular interventions guidance, diagnostics and therapy. Treated single diagnostic interventions include imaging and guidance of atherosclerosis, rhythm disorders, (micro-) vascular structure treatments, and MI characterization.

2. Photoacoustic imaging

Prior to introducing the different applications where PA imaging and sensing can make an impact, we briefly outline the principles of the imaging modality. The PA (or optoacoustic) effect describes the generation of sound waves by light absorption. When a chromophore absorbs pulsed, or otherwise time-modulated, light, the absorbed optical energy induces a transient thermoelastic expansion, which causes a pressure (sound) wave to propagate outward from the absorber (Wang 2009, Manohar and Razansky 2016). This pressure wave can be recorded by an ultrasound (US) transducer and electronic data acquisition system (figure 1(a)). Acoustic images of optical absorption can be reconstructed from the propagation delays between the light pulse and the arrival of the acoustic wave (figure 1(b)). Tissue optics determine the intensity distribution in the image (figure 1(c)).

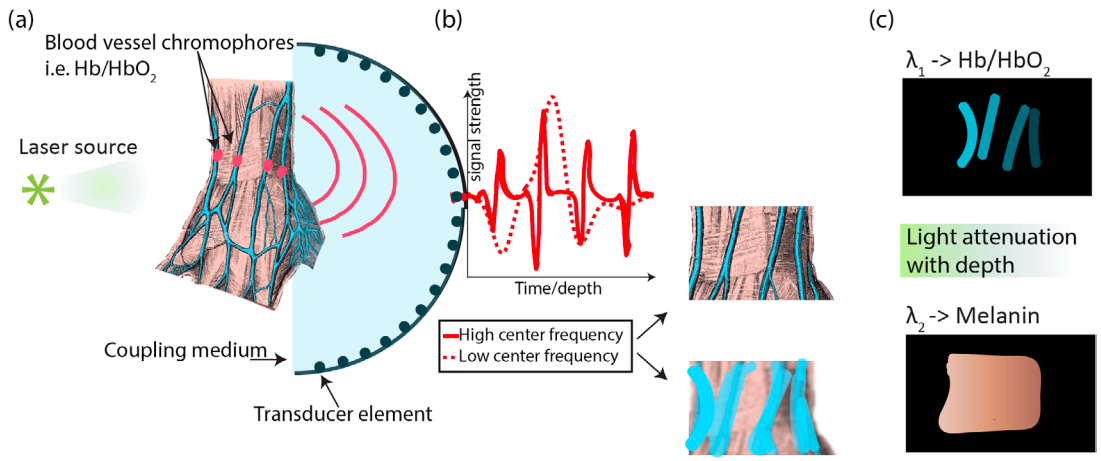

Figure 1. Principle of photoacoustic imaging illustrated. (a) A laser source shines on a targeted object and chromophores (e.g. blood vessels) absorb the light, thermoelastically expand, and emit acoustic waves which can be detected by an ultrasound transducer. (b) Typical received electrical signal at the transducer element and resulting image. Four cylindrical objects will display four characteristic waveforms; depending on the transducer bandwidth they may or may not be individually resolved (red solid versus dashed). The absorber's location can be inferred from the acoustic arrival time, and signal strength is determined by the product of the absorption coefficient and light fluence at the object location. The transducer bandwidth, geometry and illumination parameters determine the resolution of the image. (c) The optical wavelength (λ) determines the image content and penetration depth. Two wavelengths may provide contrast between e.g. blood and melanin. The signal fades with light attenuation. Hb: haemoglobin; HbO_2: oxygenated haemoglobin.

Parameters affecting the pressure wave characteristics are described by the following PA governing equation:

$$P_0(z,\lambda) = F(z,\lambda)\cdot\mu_a(z,\lambda)\cdot(z) \tag{1}$$

where p_0 denotes the source pressure generated at the chromophore location z, μ_a is the absorption coefficient of the medium, F is the local laser fluence and $\Gamma = \beta c^2/C_P$ is the Grüneisen parameter, the conversion factor of thermal to acoustic energy. In this definition, β is the thermal expansion coefficient, c is the speed of sound, and C_P is the specific heat at constant pressure. Thus, the pressure generated by photoacoustics can provide information on the tissue optical properties (through its dependency on fluence and absorption) as well as on tissue thermo-elastic efficiency properties (through the Grüneisen coefficient). Equation (1) holds under the assumption of adiabatic response, which means the pulse duration must be shorter than the acoustic transit time across the absorbing volume (stress confinement) and thermal diffusion time in that region (thermal confinement). Stress and thermal confinement are satisfied in most practical scenarios when using lasers emitting few-nanosecond pulses.

Most PA applications aim at identifying and quantifying a chromophore of known $\mu_a(\lambda)$. The dependence of equation (1) on the optical wavelength λ indicates the possibility to perform spectroscopy to retrieve μ_a. Since there are generally several different types of absorbing tissues in a given image, spectral unmixing techniques are needed to identify tissue types and quantify absorber concentrations. In its simplest form these are linear fits of the data to a set of reference spectra, but more advanced methods use computational analyses to minimize the number of wavelengths swept (Razansky *et al* 2007, Glatz *et al* 2011, Luke and Emelianov 2014). The unknown optics of the medium under investigation, in which spatially varying scattering and absorption parameters modulate the available optical energy (fluence) and thus the generated pressure, create the need for more sophisticated spectral retrieval techniques which take account of modelled tissue optics and acoustics. With carefully designed imaging sequences and analysis algorithms, chromophore concentrations (Zemp 2010, Lin *et al* 2017) in the imaged specimen can be retrieved, but also other parameters in (1), such as tissue temperature changes (Li *et al* 2015, Landa *et al* 2017), tissue optical properties (Brochu *et al* 2017, Iskander-Rizk *et al* 2018a), and potentially even thermodynamic properties. For these algorithms to work though, stable laser optical outputs or constant optical output power measurements are needed.

Instrumental requirements of PA imaging are application dependent, and as a result, various optical sources and ultrasonic detectors are reportedly used. The requirements on the optical source wavelength are dictated by the optical absorption spectra of the structures to be identified. The frequency content of the PA signal depends mostly on the size and shape (layer, cylinder, sphere) of a typical absorber (Diebold *et al* 1991): the smaller the source, the higher the generated frequencies. As large objects absorb more energy, they also generate larger pressure amplitudes, and so the ultrasonic PA spectra of mixed-size absorbers tend to be dominated by low-frequency signals, in the order of few megahertz (Diebold *et al* 1991).

3. Atherosclerosis

Obstructive vascular disorders include coronary artery disease (CAD), peripheral artery disease (PAD), and cerebrovascular disease, which may cause arterial blockages impeding the supply of oxygen and nutrients to vital organs like the heart and the brain. CAD is a manifestation of atherosclerosis- a systemic inflammatory disease of the arteries- causing plaques formation in the innermost layer of the arterial wall. Different plaques may give rise to different symptoms. A gradual narrowing (stenosis) of the vessel by growth of a fibrous or calcific plaque will, upon exertion, cause chest pain (due to cardiac ischemia); a condition called stable CAD. Sudden onset of chest pain, or chest pain at rest, is a symptom of unstable CAD or acute coronary syndrome (ACS), which is associated with thrombus formation on plaques, mostly due to the rupture of a lipid-core lesion. The most severe form of ACS is MI. The same process in the carotid arteries (in the neck) is the most common cause of stroke. Frequently, these disastrous events are the first, and possibly lethal, symptoms arising from vascular disorders, preceded by decades of accumulation of atherosclerotic plaque. In PAD, a similar disease process can affect and even endanger the lower limbs.

Catheter-based treatment of CAD consists in the implantation of a stent: a metallic (or bioresorbable polymer) vessel prosthesis that is usually introduced on a balloon. Inflation of the balloon opens the occluded vessel and expands the stent, which now supports the reopened lesion during the healing process. This procedure is called percutaneous coronary intervention (PCI). It is the standard of care for ACS, and it is also occasionally performed for stable CAD in case of severe symptoms. Imaging of atherosclerotic plaques during PCI is of interest for precisely positioning the stent to cover all of the plaque and for identifying possible lesions that may trigger new symptoms in the future. Intravascular imaging technologies use a vascular catheter to acquire image data, and deliver much higher resolution and image contrast than non-invasive methods for coronary imaging. Recent registries, meta-analyses and randomized trials have demonstrated a reduction of the relative risk of new ACS and even a reduction in cardiovascular mortality in patients that undergo PCI with intravascular imaging guidance, compared to angiography guidance alone (Jang *et al* 2014, Hong *et al* 2015, Zhang *et al* 2018).

The current model for unstable or rupture-prone plaques hypothesizes a particular morphology and composition: an eccentric plaque with a lipid-rich necrotic core that is covered by a thin fibrous cap, which is weakened by inflammatory processes. The pathology term for this phenomenology is 'thin-cap fibroatheroma' (TCFA) (Virmani *et al* 2000, 2006, Schaar *et al* 2004, Falk *et al* 2013). The heterogeneous nature of this plaque type provides several potential imaging markers for specific identification of these lesions by means of intravascular imaging (van Soest *et al* 2017).

3.1. Intravascular photoacoustic imaging

3.1.1. Plaque composition: imaging of lipids

Intravascular photoacoustic (IVPA) imaging (Jansen *et al* 2014b) is the most intensely researched application of PA imaging in cardiology. Most groups have focused on visualization of plaque lipids, as these are generally thought to be a key component of unstable or destabilizing plaques, such as TCFA (Emelianov *et al* 2008, Sethuraman *et al* 2008, Wang *et al* 2012a, Zhang *et al* 2014, Jansen *et al* 2014a, Cao *et al* 2016, Kole *et al* 2018). Being an intravascular modality, IVPA requires a dedicated imaging catheter that has the ability to deliver the excitation light and receive the PA signal. In almost all implementations, the US transducer that performs this latter task, is also used for conventional intravascular ultrasound (IVUS) pulse-echo imaging; this allows for inherent co- registration between the two modalities. IVUS can visualize the artery wall structure from its luminal border, through the vessel wall, and all the way past the outer adventitial layer, enabling the assessment of plaque burden- a powerful predictor of recurring cardiovascular events. It discriminates between soft tissues and calcified lesions but cannot reliably identify soft tissue type. IVPA adds specific contrast for tissue composition, adding chemical specificity to IVUS (figure 2). Together, these two imaging modalities provide a powerful way to image atherosclerotic plaque.

Multi-wavelength imaging has been the default approach in PA imaging of atherosclerotic plaque from the first studies onwards (Beard and Mills 1997, Sethuraman *et al* 2008). These studies demonstrated useful spectroscopic tissue type contrast. The choice of excitation wavelengths was initially limited by availability in conventional laser systems (Sethuraman *et al* 2007), demonstrating the concept but yielding mostly morphological imaging with limited specificity for the relevant tissue components.

Atherosclerotic lipids can be imaged with excitation light pulses in either of two prominent absorption bands in the short-wave infrared (SWIR) spectral region, near 1.2 μm and 1.7 μm (Wang *et al* 2010, 2012c, Jansen *et al* 2014c). Both absorption bands correspond to overtones of the C–H stretch vibration which is abundant in hydrocarbons. Imaging of lipids *ex vivo* in the artery wall of a rabbit model of atherosclerosis provided the first positive identification of a tissue component in atherosclerosis (Wang *et al* 2010). The first *in vivo* imaging experiments were likewise performed in a rabbit aorta (Wang *et al* 2012a). In the longer 1.7 μm wavelength window, blood scattering is sufficiently small that imaging lipids in the artery wall with luminal blood is possible (Wang

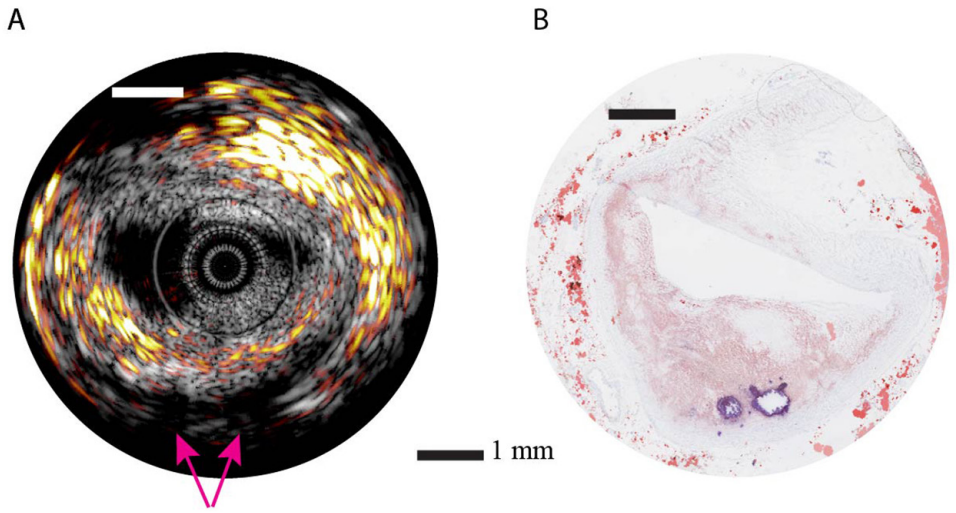

Figure 2. IVPA image of human coronary artery *ex vivo* (a) and its corresponding Oil red O (ORO) histology evaluation (b). The pink arrows correspond to the calcification stained in purple in (b). The PA signal in yellow–orange–red scale in (a) clearly identifies the lipid rich plaque within the vessel wall thickening. Reprinted from Iskander-Rizk *et al* (2018c); *Copyright © 2018 Society of Photo-Optical Instrumentation Engineers (SPIE).*

et al 2012b). Water absorption limits the imaging depth to a few millimetres (Jansen *et al* 2013). At 1.2 μm, blood optical absorption is lower but the overall optical attenuation due to scattering is strong, reducing the energy available for generating the PA signal (Wang *et al* 2012c).

The first IVPA images of human specimens (Jansen *et al* 2011) highlighted the lipid content of advanced atherosclerosis by differential imaging at wavelengths on and off the main lipid absorption peak. Follow-up analyses of the detailed absorption spectra revealed variability in the absorption spectrum of plaque lipids, and identified differences in the absorption spectra between the sterol-rich content of atherosclerosis and the fatty-acids in adipose tissue surrounding the vessel (Jansen *et al* 2014a). The spectral contrast is sufficiently robust to provide contrast between peri-adventitial fat and plaque lipids with only two wavelengths (Jansen *et al* 2013, Wu *et al* 2015) (figure 3), capitalising on slight shifts in the resonant frequency depending on the molecular conformation of the vibrating bond (Holman and Edmondson 1956). Using the same spectral band (1.6–1.8 μm), spectroscopic PA imaging differentiated collagenous tissue from lipids (Wang *et al* 2012c).

In a nutshell, the current advances in IVPA/US lipid-plaque imaging are close to bringing this method to (pre-)clinical applications. Imaging *in vivo* was demonstrated by multiple groups in various animal models (figure 4(a)) (Wang *et al* 2012a, Wu *et al* 2017, Cao *et al* 2018, Kole *et al* 2018) with different catheter designs (Karpiouk *et al* 2012, Wu *et al* 2014) through blood (Wang *et al* 2012b). Specificity to human atherosclerotic plaque was shown with *ex vivo* specimens (Jansen *et al* 2014a), suggesting that the achievements shown *in vivo* on animal models could potentially be achieved on humans. Emphasizing on the latter, the miniaturised catheters were also shown to be flexible enough to be navigated through swine coronaries (Wu *et al* 2017); which is the closest coronary anatomy to human. Only two steps remain prior to the design of studies validating the use and advantages of the imaging method for disease monitoring and intervention guidance. These are intracoronary IVPA/US *in vivo* imaging of atherosclerosis, and demonstration of real time *in vivo spectral* IVPA/US imaging for defined plaque feature identification.

3.1.2. Plaque composition imaging: other imaging targets

Inflammation is a prominent mechanism driving atherosclerosis. Interventions targeting systemic suppression of inflammatory response have been shown to reduce cardiovascular events and CV mortality (Ridker *et al* 2017). Inflammation, in conjunction with lipid content, may provide important information about the event risk of an atherosclerotic plaque and consequently, could play a role in guiding device- or drug-based interventions. These features of atherosclerosis have been visualized with the aid of exogenous contrast agents, as recently reviewed in another contribution to this Focus Issue (Sowers and Emelianov 2018).

Inflammation is an innate response to injury or stress and is mediated by a complex of signalling molecules and cells. The most prominent of these inflammatory cells are macrophages, which play important roles in plaque biology, interacting with lipid transport and sequestration, efferocytosis, and weakening of connective tissue by secretion of matrix-metalloproteinases (MMP) (Silvestre-Roig *et al* 2014). Macrophages themselves do not exhibit a clear specific optical absorption feature. Both gold nanoparticles (Wang *et al* 2009) and the FDA approved indocyanin green (ICG) dye (Bui *et al* 2017), taken up by macrophage cells through endocytosis or

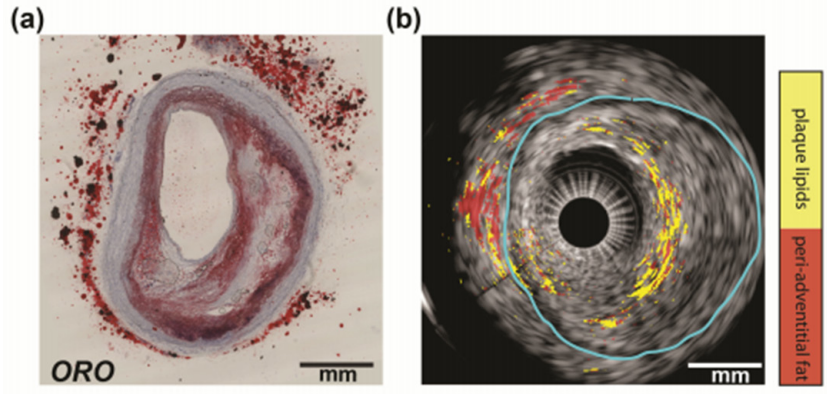

Figure 3. Spectral IVPA/US of a human coronary artery *ex vivo* and its corresponding histologic slice (ground truth). Two wavelengths, 1718 nm and 1734 nm, are sufficient to discriminate plaque lipids from peri-adventitial lipids. The blue line delineates the media/adventitia border. Reprinted from Wu *et al* (2015), *Copyright © 2015 Optical Society of America.*

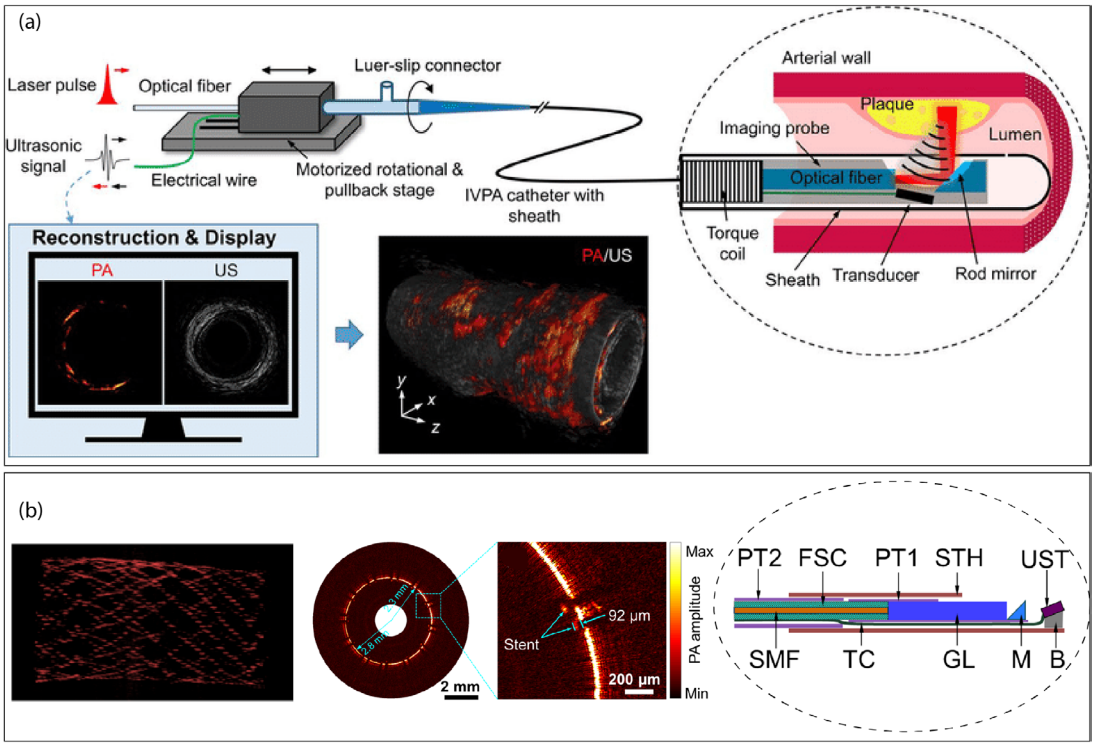

Figure 4. (a) *In vivo* imaging of a rabbit aorta using a quasi-collinear/beam offset catheter design; reprinted from Cao *et al* (2018), *with permission; © CC BY 4.0.* (b) Optical resolution intravascular photoacoustic imaging of a stent *ex vivo*. The catheter design focuses the light through the use of a grin lens; reprinted from Bai *et al* (2014), *with permission © 2014 Bai et al.* FSC: flexible stainless steel coil; PT1: polyimide tube 1 with an inner diameter of 0.7 mm; PT2: polyimide tube 2 with an inner diameter of 0.74 mm; STH: stainless steel tube housing; UST: ultrasonic transducer; SMF, single-mode fibre; TC: transducer cable; GL: gradient-index lens; M: micro-prism; B: metal base.

phagocytosis were shown to enable PA imaging of macrophages in *ex vivo* animal arteries. *In vivo* imaging has yet to be demonstrated, which may be complicated by the choice of wavelengths, 700 nm, 750 nm and 805 nm, that are highly absorbed by haemoglobin. Tests on gold nanorods cytotoxicity showed that the particles do not particularly alter cellular viability in comparison to control cultures (Qin *et al* 2013, 2016, Ricles *et al* 2014). Other PA contrast agents were engineered to identify the presence/absence of metalloproteinases as a marker for plaque vulnerability. Both targeted gold nanorods (Qin *et al* 2016) and MMP-sensitive activatable fluorescent probe (Razansky *et al* 2012) were shown to image MMP in atherosclerotic plaques *ex vivo*.

Since metals are efficient optical absorbers, IVPA can also image stents as a means of evaluating stent apposition during PCI. In Bai *et al* (2014), a miniature flexible catheter capable of high-resolution PA imaging was built. The results show a better point spread function (PSF) than obtained with IVUS, with a transverse resolution of 19.6 μm (figure 4(b)).

3.1.3. Experimental considerations and device design

IVPA can potentially target several of the plaque features of interest: lipids, macrophages and intraplaque haemorrhage (Arabul *et al* 2017). The complementarity with IVUS adds the capability of evaluation of plaque morphology and even stiffness (Schaar *et al* 2003). A combined IVUS/IVPA imaging system is clearly desirable over either modality alone. In general, intravascular images are acquired by stacking arterial cross-section images obtained at different locations while pulling back the catheter from distal to proximal in the artery. Virtually all experimental intravascular catheter prototypes presented to date are side-looking (i.e. the optical and acoustic beams are directed sideways from the catheter in the artery lumen) and image the arterial wall, using a single-element configuration that is rotated around its long axis (Li and Chen 2018). A plastic sheath confines the rotating imaging core to provide guidewire compatibility and prevent tissue damage. In the following paragraphs, we discuss some of the key elements of an IVPA/US imaging system.

The rotary scan sequence of common IVPA implementations requires at least one laser pulse for each A-scan. Faster lasers would allow for averaging and thus improved SNR. Thus far the fastest imaging frame rate achieved was 30 fps using a 10 kHz pulse rate laser source at 1064 nm (VanderLaan *et al* 2017) *ex vivo*. Parallel detection and electronic beam scanning on multiple transducers can in principle speed that up to hundreds of frames per second (Wu *et al* 2019). However, the highest frame rate demonstrated *in vivo* was of 20 fps (Wu *et al* 2017) based on a rotary scan implementation.

The choice of all materials in the beam path, the sheath material in particular, is governed by the optical and acoustic compatibility at the operating wavelengths and frequencies. An ideal catheter sheath minimizes optical absorption, acoustic attenuation, acoustic reverberation and maximizes flexibility. The fact that lipid imaging relies on C—H absorption- a molecular bond that occurs prominently in many polymers- severely complicates this quest. Thus far, polyurethane and specific polyethylenes were found to have acceptable ultrasonic and optical transmission at wavelengths around 1.7 μm (Cao *et al* 2018, Iskander-Rizk *et al* 2018c), but do leave room for improvement. Use of more wavelengths for access to more plaque features is likely to exacerbate this issue.

Lipids occur in tissue in different forms, such as intra-cellular and extra-cellular droplets, dispersed in cell and organelle membranes, and as cholesterol crystals. PA imaging relies on the acoustic wave emitted from an absorbing object upon thermoelastic expansion after exposure to a short laser pulse. The well-known dependence of frequency content and amplitude on the size and shape of the PA source applies, which explains why the PA signals from the lipid-rich plaques have the highest energy in the lower frequency band ($<$8 MHz) (Daeichin *et al* 2016b). Thus far, in all the IVPA/US catheter prototypes the US element was optimized for the resolution requirements set by IVUS imaging, using centre frequencies of 30 MHz and higher. Transducers of lower centre frequency ($<$20 MHz) may benefit the SNR of IVPA images. These need to fit within the size required for coronary catheters ($\leqslant$1.1 mm outer diameter). Approaches such as all-optical transduction (Mathews *et al* 2018) and dual-element configurations (Ji *et al* 2015) may be successful in the future in achieving the required bandwidth for combined IVUS/PA imaging.

Safety of currently proposed imaging systems is necessary before any potential use on humans. An irradiation limit exists at which laser-tissue interaction becomes harmful. Maximum permissible exposure values are well established for some organs such as the skin or the eye, but are less known for other tissue types. Design for safety should take into account the illumination wavelength, the laser pulse repetition frequency (PRF), power and pulse duration, as well as the system's pullback and rotation speed. Studies on smooth muscle, macrophage and endothelial cell cultures *ex vivo* demonstrated that the typical exposure levels used in IVPA imaging were not harmful to the cells (tested wavelengths: 1064 nm, 1197 nm, 1720 nm) (Sowers *et al* 2018). Likewise, *in vivo* IVPA imaging in the iliac artery of an Ossabaw swine showed no tissue damage through post-experimental histology evaluation of imaged and control vessels (Kole *et al* 2018). It is also important to demonstrate catheter deliverability, mechanical and electrical safety.

3.2. Non-invasive imaging of atherosclerosis

Evaluating the progress of atherosclerosis could be non-invasively performed on carotid or other peripheral arteries. Several features of plaques are similar between the coronary and carotid arteries: thrombi, macrophage infiltration, TCFA cap thickness, lipid content, and so we can expect to see the same features in the images. The imaging system is fundamentally different, though: the peripheral arteries are accessible to linear-array-based US imaging. PA imaging can be performed using the same transducer, such that parallel detection on many or all elements results in a full PA image from one laser pulse (subject to SNR requirements which may encourage averaging of multiple pulses), where catheter-based imaging required at least one pulse for each A-line.

For carotid imaging, a commercially available US array is positioned on the neck of the patient to receive the PA signals from the carotid artery as well as to perform routine US (B-mode and Doppler) imaging. Light can be delivered externally, next to the transducer array on the side of the neck, which results in a longer light path, and thus more attenuation, but allows the use of larger pulse energies (figure 5) (Dima *et al* 2014). Alternatively, the

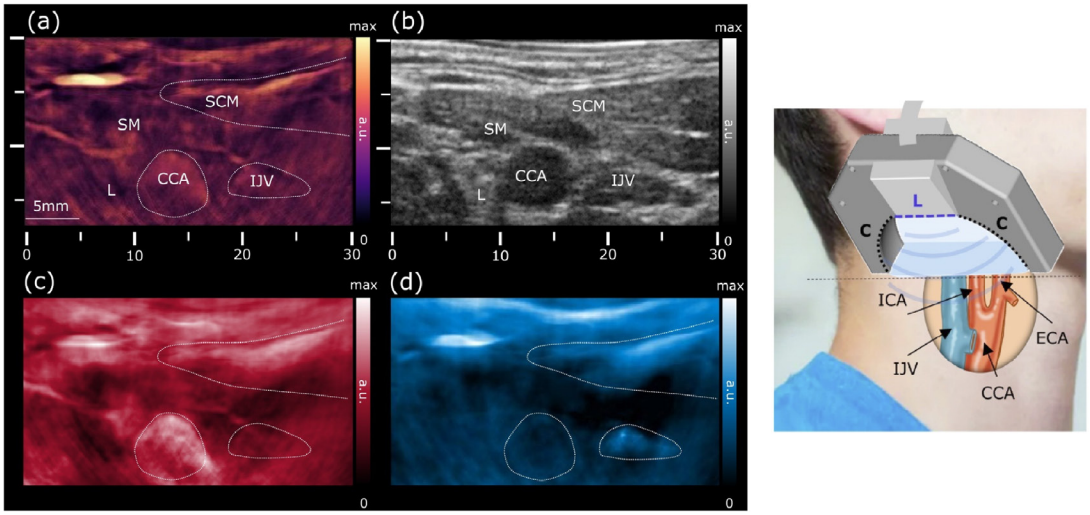

Figure 5. Carotid PA/US imaging configuration setup and resulting images with illumination source and acoustic transducer co-located on the neck. (a) PA image at 800 nm the main structures observed are delineated and annotated. (b) Corresponding B-mode US image. (c) Spectrally unmixed image to map oxygenated haemoglobin. (d) Spectrally unmixed image to map deoxygenated haemoglobin. SCM: sternocleidomastoid muscles; SM: strap muscle; ICA: internal carotid artery. ECA: external carotid artery; IJV: internal jugular vein; CCA: common carotid artery. Image reprinted from Mercep *et al* (2018), with permission, *Copyright © 2018 The Authors, CC BY-NC-ND.*

illumination source can be positioned in the pharynx and/or oesophagus (figure 6) (Kruizinga *et al* 2014), leading to a more efficient delivery but a smaller illuminated volume.

In vivo PA imaging of the carotid artery and jugular vein was demonstrated on healthy volunteers (Dima and Ntziachristos 2012, Mercep *et al* 2018, Ivankovic *et al* 2019). These show the feasibility of generating sufficient signal from the target vessels, at an imaging depth of 12–15 mm through the skin layers with external illumination, showing features such as the carotid bifurcation. Use of an ultrasonic transducer centred at about 5 MHz in combination with an excitation light of ~800 nm and of fluence compatible with optical exposure limits, enabled the imaging of multiple structures such as the jugular vein and the strap muscles (figure 5). The chosen wavelength of 800 nm may, however, not be ideal for detecting atherosclerotic plaque, especially near the large blood pool in major vessels. Such issues may potentially be resolved by spectral unmixing. PA images at seven wavelengths between 700 and 850 nm distinguished between arterial and venous blood (figure 5) (Mercep *et al* 2018), but could potentially also contain contrast for plaque haemorrhage. Indeed, PA signals of *ex vivo* carotid plaque specimens at 808 nm correlated with intraplaque haemorrhage on histology (Arabul *et al* 2017). In addition, four wavelengths between 808 and 980 nm distinguished between cholesterol crystals, porcine blood and thrombus in an *ex vivo* phantom using blind source spectral unmixing methods (Arabul 2018). Imaging results reported on intraplaque haemorrhage would however prove more valuable for clinical translation if demonstrated on vulnerable plaque specimen with luminal blood.

Other studies imaged atherosclerotic carotid arteries at relevant lipid differentiating wavelengths. PA imaging of a human carotid plaque specimen was mimicked using a phantom that replicated the anatomy of the neck, and explored illumination through the pharynx (Kruizinga *et al* 2014). They showed feasibility of imaging plaque lipids at the illumination wavelengths around 1200 nm, using safe optical fluence levels. At 1200 nm, external illumination through the skin would not be realistically achievable, due to the long optical path length and high absorption and scattering of skin. However, illumination through the pharynx at 1200 nm should be in practice achievable, though full carotid, wall-to-wall illumination and *in vivo* imaging, needs to be confirmed.

3.3. Perspective on therapeutic interventions and risk assessment

From a cardiovascular intervention point of view, the presented research, shows that IVPA/IVUS is a strong candidate to determine optimal stent placement, stent sizing, and for pre-emptive treatment of high-risk sites during a PCI. Angiography can often identify the culprit lesion, but the addition of IVPA/US may help to define the entire implicated segment, and to identify other (asymptomatic) vulnerable plaques. This comprehensive assessment of the disease severity and extent within the artery may inform a better (pre-emptive) treatment plan. IVPA imaging can image plaque composition, while the structural information from IVUS relates them to the overall vessel wall architecture. The multimodal structural and chemical information provided by IVPA/US has the greatest potential for assessing plaque vulnerability to rupture. In clinics, other imaging technologies exist for diagnostic assessment of coronary atherosclerosis, such as IVUS, optical coherence tomography (OCT) and near-infrared spectroscopy (NIRS). However, none of these has adequate sensitivity for all plaque features that

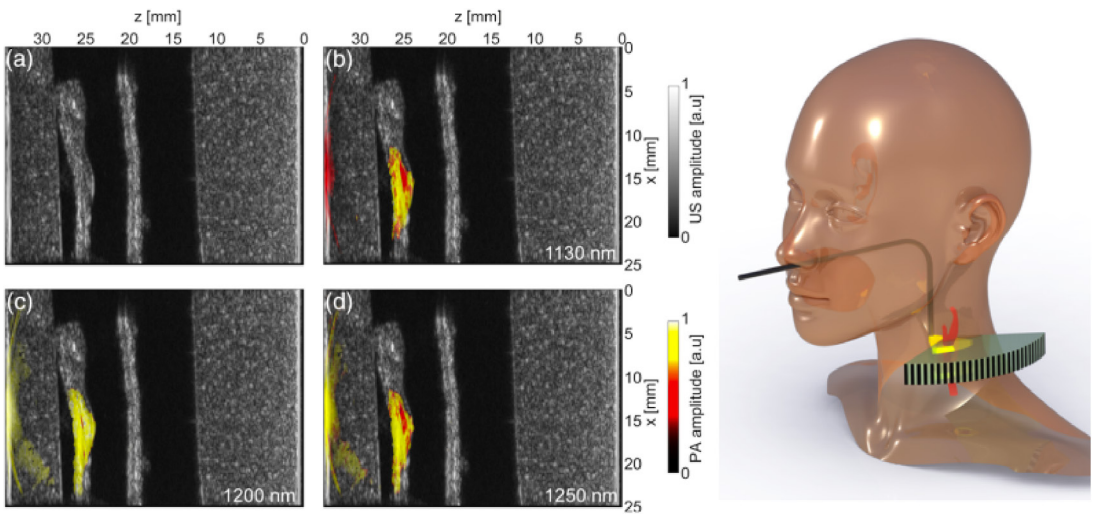

Figure 6. Carotid PA/US imaging configuration setup and resulting images with the illumination source located in the pharynx and the acoustic transducer on the neck. (a) US B-mode image of a neck phantom. (b) PA image at 1130 nm overlaid on US. (c) PA image at 1200 nm overlaid on US. (d) PA image at 1250 nm overlaid on US. Plaque lipids signals are located based on spectral unmixing from the surrounding collagen signals. Image reprinted from Kruizinga *et al* (2014), with permission, © *Copyright 2018 Society of Photo-Optical Instrumentation Engineers (SPIE)*.

are known to correlate with vulnerability. For instance, plaque size can be determined by IVUS and lipid content can be assessed by IVPA as discussed in the previous section. Measurement of cap thickness, which requires an imaging resolution of <50 μm, has not been demonstrated but is not beyond the realm of possibility (Bai *et al* 2014, Li *et al* 2012).

The eventual proof of clinical efficacy of an IVPA/US imaging would be a demonstration of fewer ACS cases in patients undergoing IVPA-guided PCI compared to those receiving standard of care treatment. Such trials are now emerging with IVUS, more than 20 years after the clinical introduction of the technology (Hong *et al* 2015, Zhang *et al* 2018). Until then, intermediate steps would include a quantitative characterization of culprit lesions compared to non-culprit sites, and a natural history study documenting plaque changes over time. These trials with imaging endpoints will serve to define the IVPA-based treatment criteria that can be evaluated in an outcomes-based trial.

Non-invasive imaging may serve dual role: since carotid atherosclerosis is the most common cause for stroke, detailed imaging of plaque content may improve risk assessment for patients. In today's practice, imaging technologies such as echo, x-ray CT and MRI are used for this purpose, but these are limited in their ability to predict future events and can be expensive. PA imaging may provide a highly chemically detailed image of plaque composition that may augment this picture. Another potential application may be the monitoring of systemic atherosclerotic disease status. Atherosclerosis in peripheral arteries have been identified as a proxy for coronary artery disease, and the carotid artery has been particularly popular for this purpose (Craven *et al* 1990, Cohen *et al* 2013).

4. Arrhythmias: atrial fibrillation

The field of interventional electrophysiology has only started to mature over the past 30 years, pushed by the advances made in intracardiac recording technology (Myat *et al* 2012). Interventional electrophysiology has opened the cardiac electrophysiology field to new curative approaches as opposed to traditional solutions concerned only with the management of the disease and pharmacology. Medication for atrial fibrillation consists of anti-coagulants to prevent blood clots, and decrease risks of ischemic stroke. Other prescribed drugs are anti-arrhythmic treatments to control the heart rhythm. Research aiming to elucidate heart rhythm disturbance mechanisms has led to identification, classification and better understanding of different types of arrhythmias, unravelling different diagnosed types, each requiring its own specific therapeutic approach. For instance, bradyarrhythmias (lower than optimal heart rate) are often treated with pacemaker implants. Tachycardias (fast or irregular heart rates) often require ablation: induced tissue scarring to stop aberrant conductive pathways. While treatment of tachycardias initially required an open-chest surgery, it nowadays can be performed percutaneously with minimal risk in a procedure named catheter-based ablation. Such procedures rely heavily on imaging technology and intracardiac electrophysiological mapping for guidance and treatment delivery, and this is where PA imaging can make an impact.

Atrial fibrillation is one such tachycardia. The pathology of atrial fibrillation is associated with other heart diseases such as atherosclerotic heart disease, valvular heart disease and diabetes mellitus. These comorbidities contribute to an increased mortality rate (Bajpai *et al* 2007). Factors predisposing the disease onset include excessive alcohol consumption, smoking, obesity, diastolic dysfunction and ageing. Symptoms affect patient's quality of life and may include chest pain, shortness of breath, palpitations, fatigue or heart failure. Atrial fibrillation is also associated with an increased risk of stroke and thromboembolism, which could be fatal. The prevalence of atrial fibrillation is predicted to increase, due to an ageing population and the mutually reinforcing CVD health factors discussed above (Chugh *et al* 2014).

4.1. Catheter-based ablation as a treatment for atrial fibrillation

Atrial fibrillation can nowadays be treated with catheter-based ablation, mostly obviating the complicated open surgical intervention. It is by far one of the most complicated arrhythmias to treat, with procedures often lasting longer than 4 h. Since atrial fibrillation is the most common sustained arrhythmia, affecting 0.5% of the global population in 2010 (Chugh *et al* 2014), with the highest complication rates, research into PA guidance of catheter-based ablations mostly targeted procedures for atrial fibrillation.

Pharmaceutical management of the disease is nowadays being shown to be inferior to a curative ablation approach (Srivatsa *et al* 2018). In a minimally invasive procedure, an ablation catheter as well as other electrophysiological catheters (e.g. for recording surface potentials), are inserted through the femoral vein to the atria to deliver treatment locally under fluoroscopy and echocardiography guidance. In catheter-based ablation for atrial fibrillation, the targeted ablation tissue is usually at the ostia of the pulmonary veins in the left atrium. Catheter-based ablation procedures for atrial fibrillation often last longer than 4 h.

In this procedure, technology is crucial. Long procedures under fluoroscopy guidance lead to excess exposure of radiation for the patient. Insertion of the catheter sheath from the right to the left atrium is performed under intracardiac echography (ICE) imaging. Guidance of the procedure relies on electro-anatomical maps (EAM), which identify the irregular conductive pathways and determine the regions to be treated. Such EAMs are made by tracking the position of the electrophysiology catheter as it is dragged along the atrial wall to record local electrograms. Real-time feedback on treatment evaluation relies on electrophysiological catheters (for instance, a lasso catheter) to determine cessation of conductivity as well as on sensors at the ablation catheter tip for feedback on energy delivery. These sensors comprise, among others, temperature, impedance and contact-force sensors which can indirectly predict the efficacy of conversion of the energy delivered into the tissue, with the aim to induce scarring.

Feedback on energy delivered is important. In about 4.5% of the procedures, complications arise due to the ablation of untargeted areas: excessive energy delivery (over-ablation) reaching the oesophagus or the phrenic nerve causing serious injury to the patient (Steinbeck *et al* 2018). Lesion size is also important because it is believed that the low interventional success rate of 60%–70% is due to incomplete ablation (under-ablation), (Ouyang *et al* 2005, Ganjehei *et al* 2011). Gaps between lesions, healing of tissue oedema, shallow lesions and difficulties in ectopic foci identification will lead to tissue reconduction. Thus, the cornerstones of catheter-based ablation intervention success are assumed to be (1) full and correct identification of ectopic foci (2) transmural ablation lesion formation and (3) continuous lesion formation for electrical isolation.

4.2. Photoacoustic imaging for ablation lesion characterization

The major complications happening during the catheter-based ablation procedures are related to control of energy delivery, and many innovative solutions aim to provide a means to better control the ablation, in order to make the catheter-based intervention faster and safer. The types of feedback provided by today's technologies (e.g. temperature, contact impedance power delivered, and duration of energy delivery settings), can only help the cardiologists to *estimate* the size of the lesions they have created. To this day, no commercially available technology provides full visualization and characterization of ablation lesions' long-term electrical functionality, and its lateral and transmural extent. It is however of extreme importance for the electrophysiologist to follow the progress of the tissue changes induced by the ablation process. Direct monitoring of energy delivery and visualization of its effect on tissue changes could improve the outcome of the procedure (Wright 2015).

4.2.1. Photoacoustic tissue contrast

Initial studies of visualizing RF ablation lesions with PA imaging showed very promising results (Bouchard *et al* 2012, Dana *et al* 2014, Pang *et al* 2015, Iskander-Rizk *et al* 2018a). Governed by equation (1), the detected pressure as a result of transient absorption depends mainly on the tissue optical properties. To visualize lesions, it is thus necessary to determine optical wavelengths that exhibit robust absorption contrast between the lesion chromophores and the surrounding tissue. The signal contrast may visualize treated areas among healthy tissue. First report of spectral contrast between ablated swine myocardium and healthy ventricular myocardium was shown in a PA spectroscopic study (Bouchard *et al* 2012). From then on, other groups have further confirmed

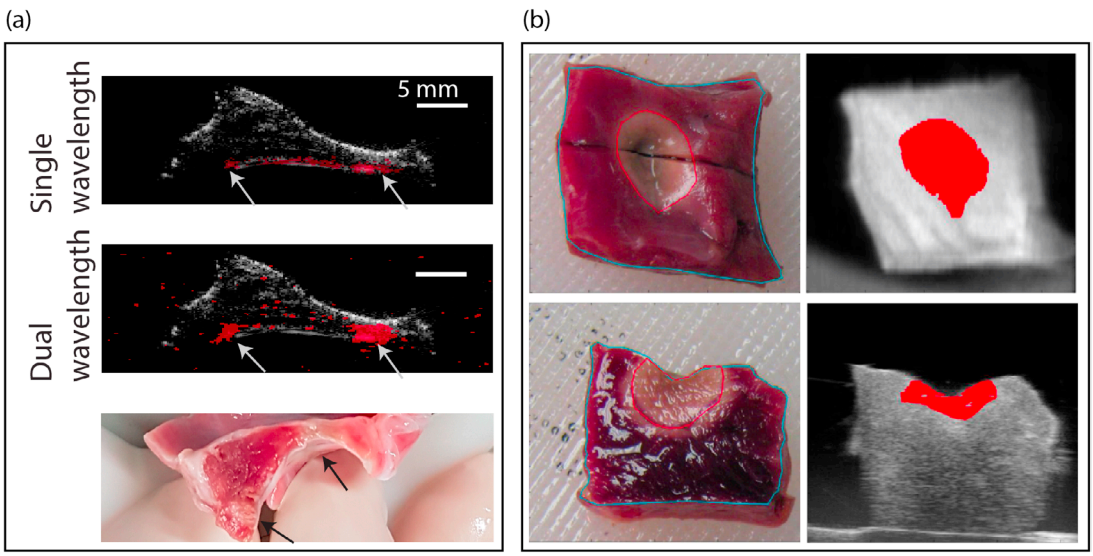

Figure 7. Photoacoustic imaging of ablation lesion. (a) USPA images of ablated tissue using two imaging schemes and corresponding ground truth in photograph. Arrows point at the lesions. Reprinted from Iskander-Rizk *et al* (2018a), © *2018 Optical Society of America.* (b) Spectroscopic imaging on porcine ventricular tissue. Figure reprinted from Dana *et al* (2014) *Copyright (2014), with permission from Elsevier.*

capability of lesion visualization of cardiac tissue *ex vivo* in 3D. Imaging contrast was shown for both ventricular (Dana *et al* 2014) as well as atrial tissue (Iskander-Rizk *et al* 2018a) (figure 7), with imaging depths reaching up to 6 mm (Pang *et al* 2015). Though imaging contrast was shown on swine models, the results are expected to translate to human tissue because of the optical similarity between the two, as was shown in Singh-Moon *et al* (2015).

PA imaging could thus potentially be used for both ablation of supraventricular arrhythmias, as well as ventricular ones. Nonetheless, a systematic study on signal strength and contrast for different tissues and cardiac anatomic sites is still needed. Endocardium, myocardium and epicardium thickness, smoothness and orientation vary with location, affecting tissue scattering and optical propagation paths.

It is important to bear in mind that all PA studies of RF ablation lesions to date were on non-vascularized porcine tissue. Haemoglobin being the most dominant chromophore in the near infrared range could affect the lesion imaging capability, in terms of image contrast, image depth (Gandjbakhche *et al* 1999) and thus lesion delineation and correct identification. To contravene this potential drawback, different imaging methods were proposed. For instance, spectral correlation methods were used to differentiate background signal from lesions focussing on the peak signature of haemoglobin at 760 nm (figure 7(b)) (Dana *et al* 2014). A dual wavelength ratiometric technique offered a more simplistic approach to discriminate lesion signals from the surrounding background (figure 7(a)). It was nevertheless highly efficacious, achieving 97% diagnostic accuracy for precise detection of RF ablation lesions against a variety of background conditions (different locations and wall thicknesses, blood at different oxygenation levels) (Iskander-Rizk *et al* 2018a). Though promising, further studies are needed to prove robustness of these methods to separating blood-generated PA signal from the lesion PA signals, as well as to quantify the effect of optical propagation and optical deposition in perfused tissue.

Clinically-approved techniques other than RF ablation include balloon-based methods, such as cryo-ablation which applies extreme cold to locally freeze the tissue (Schmitt *et al* 2006), or laser ablation and coagulation (Dukkipati *et al* 2013). Studies have shown the equivalence in histology of the lesions formed through different techniques (Aupperle *et al* 2005). One may therefore expect that the lesion-specific chromophores be the same, regardless of the method of ablation. It is important, however, to consider that the strength and polarity of the PA signal are temperature dependent, because of its dependence on the thermal expansion coefficient. This dependence may affect the generalization of results obtained with RF ablation to other energy modalities. With proper characterization, the temperature dependence of the signal could also be used for in-depth temperature profiling (Rebling *et al* 2018). Currently, cardiologists rely on a surface measurement which is of limited use with flushed catheters, or when underlying vessels cool the tissue. This is an interesting feature to explore as the tissue temperature is a key factor for the quality of the lesion that is produced.

4.2.2. Instrumentation development

Different imaging configurations were evaluated in published studies to date. PA monitoring of cardiac ablation needs to operate in or on the blood-filled cavities of the heart. The optical source and acoustic transducers have

been realized as one integrated device (Pang *et al* 2015), but separated optical and acoustic configurations have also been demonstrated (Dana *et al* 2014, Iskander-Rizk *et al* 2018a). Dual modality, US-PA images were formed using transducers of various centre frequencies, extending from low frequencies (<3 MHz) to high frequencies (21 MHz), also covering the ICE bandwidth range of ~6 MHz. Imaging was feasible for different imaging conformation with the transducer positioned at different locations with respect to the tissue and illumination source, showcasing that PA has the potential to image the ablation process for different cardiac locations spanning from the trans-septal wall to the pulmonary veins.

PA imaging and RF ablation with a dedicated PA-enabled ablation catheter delivers light directly at the ablation site (figure 8) (Rebling *et al* 2018, Iskander-Rizk *et al* 2018b). An ICE catheter, which is currently already in routine use, may be used to receive the PA signals. These can be displayed as an overlay on the ICE images. This configuration offers the advantage of delivering light directly at the ablated site, minimizing the impact of blood. It has the potential for becoming a drop-in solution, since minimal changes to current practice would be needed. Another design (Nikoozadeh *et al* 2012) consisted of an ablation catheter that enables both PA and US imaging, but it was not evaluated for tissue ablation imaging yet. From a manufacturability point of view, PA-enabled catheters at a size that is compatible with today's interventions appear to be feasible.

4.3. Looking forward to electrical mapping

Electrical mapping is the cornerstone of interventional electrophysiology. Not only is it the base for syndrome diagnostic and treatment planning but it also has potential of being a tool to predict future fibrillary substrates. A popular adage claims that 'atrial fibrillation begets atrial fibrillation', referring to the fact that AF, when persistent for a long period of time (>24 h), has the capability of regenerating itself after termination. This is due to the electrophysiological remodelling induced by the persistence of the AF. In such cases, cells may display shorter refractory periods than normal and may induce AF again. This mechanism means it is more difficult to restore the sinus rhythm in prolonged AF and identification of such substrate might be of interest to the cardiologists for preventive measures. A potential advantage of imaging of electric potentials over current electrode-based potential measurements is the extension to volumetric mapping. Unravelling endocardial to epicardial signalling is indeed an important feature for current electrophysiology research (de Groot *et al* 2016).

In absence of native electrical contrast, PA imaging methods are not able to image cardiac electrophysiological potentials intrinsically. However, with the use of PA sensitive contrast agents, it may be possible to visualize tissue electric potential variations. Indeed, PA signals were found to be correlated to calcium dynamics of cardiomyocytes in culture when using a dye named Arsenazo III (Dana *et al* 2016). Electrical polarization of the muscle cell being strongly related to cellular calcium flow, positions this dye-based imaging method as a contender for cardiac electrophysiological potential monitoring. *In vivo* application of this contrast agent will however be limited by its absorption in the visible range, which is difficult to reconcile with imaging through blood or in perfused tissue. PA voltage sensitive dyes were mostly investigated on brain tissue. Engineering of a near-infrared PA voltage-sensitive dye improved the depth at which brain tissue electrical potentials could be tracked (Zhang *et al* 2017). In addition to that, electrical potentials at the surface of the mouse brain were successfully disentangled from tissue hemodynamic signals using spectroscopic methods (Rao *et al* 2017). This latter feature is potentially also useful in cardiac tissue to distinguish between perfusion and contractility signalling, while the former is likely to improve imaging of cardiac signalling at depth. Today, the research on PA voltage mapping of cardiac tissue is sparse, but with the right voltage sensitive dye, electrical mapping is not beyond the limits of PA technology. Current challenges lie in the engineering of the dye's absorption wavelength and dynamics to optimize for PA spatio-temporal electric potential resolution at various depths. Needless to say that cytotoxicity and flushing mechanisms must also be taken into account.

5. Vascular imaging

Most of the PA imaging literature capitalizes on blood as a dominant chromophore and target contrast. Blood is the main biological absorber of light in the visible and near-infrared wavelength range and stands out from the other background biological absorbers with spectroscopic contrast between oxygenated and deoxygenated haemoglobin. An innovation in cardiovascular and intensive care medicine that capitalizes on this contrast develops a PA monitoring tool of the oxygen saturation of the venous blood in the pulmonary artery by transoesophageal illumination and acoustic reception (Herken *et al* 2016, Li and Tearney 2017). Extension of the functionality of such a device to guidance of atrial ablations is conceivable.

Microvasculature is a popular imaging target in animal models (Hu *et al* 2009, Hu and Wang 2010, Beard 2011) and humans (Aguirre *et al* 2017) through focused excitation or reception of signals. Nonetheless, high resolution imaging of vasculature works only superficially, is time consuming, and requires bulky scanners. The high resolution of such systems can be put to use for PA flow cytometry (Galanzha and Zharov 2012), demonstrated *in vivo* on small animal models to detect and differentiate between circulating red blood cell aggregates,

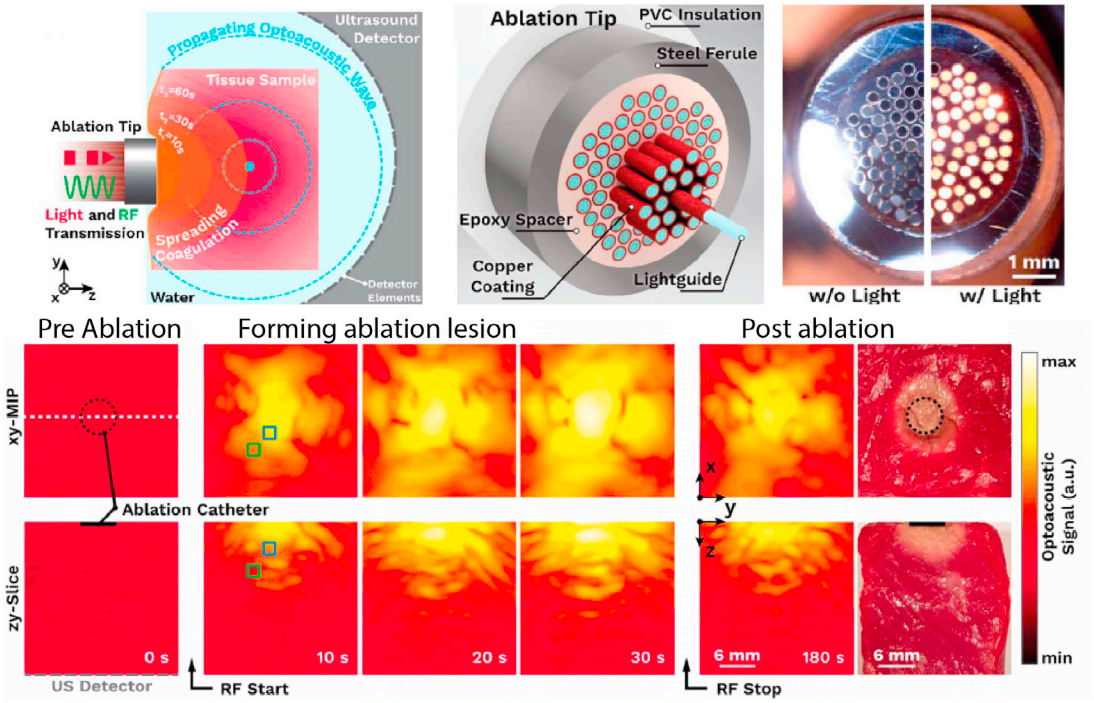

Figure 8. Photoacoustic-enabled ablation catheter. The optical fibres are coated with copper to deliver both RF current and laser light. Monitoring of lesion formation was also achieved with the presented prototype. Reprinted with permission from Rebling *et al* (2018) © *2018 Optical Society of America*.

white blood cell aggregates, and platelets (Galanzha and Zharov 2011, Galanzha *et al* 2011). Moreover, the technique was used to monitor the formation of blood clots during surgical procedures (Galanzha *et al* 2011, Juratli *et al* 2016, 2018). Other applications are new *in vitro* diagnostics for various blood conditions, including the ability to sort cells with the recent feasibility demonstration of PA circulating cell focusing (Galanzha *et al* 2016).

The main application of these techniques lies in the monitoring of intensive care unit patients. The measured parameters directly relate to blood coagulability and hemodynamic stability, which is frequently compromised in patients with acute cardiovascular disorders, and so these data may in fact inform interventions in that population in the future. Other reviews have extensively discussed PA flowmetry and its applications (Tuchin *et al* 2011, Galanzha and Zharov 2012, van den Berg *et al* 2015).

5.1. Myocardial infarct

A MI is the name given to the irreversible damage to the myocardium by prolonged ischemia. The damage can span from loss of contractility to necrosis as a result of a coronary artery blockage. Myocardial tissue necrosis may lead in the long term to heart failure. At the onset of symptoms, the first tests to confirm a myocardial infarct are a diagnostic ECG to localize the area of infarct and a blood test to determine presence of biochemical markers for cardiomyocyte death. Medication is given to dilate the blood vessels and minimize thrombus formation. Emergency or staged PCI, usually with stent placement, are the next steps of treatment. Several new mitigating or curative interventions are currently in development, including endovascular hypothermia application in conjunction with PCI (~33 °C, cold saline before reperfusion), which may reduce the infarct size (Reddy *et al* 2015). Several stem cell therapy approaches have also been proposed but remain highly speculative.

There are no PA imaging studies to date that show concrete translational potential in the localization and treatment guidance of myocardial infarcts in humans. Full murine heart perfusion or oxygenation (Zemp *et al* 2008, Lin *et al* 2017, Lv *et al* 2018, Mukaddim *et al* 2018), which are surrogate estimates of MI features, corresponded well with measurements provided by left ventricular ejection fraction and MRI/SPECT images. However, the demonstrated non-invasive illumination, feasible through the thin murine chest wall, would not translate well to the human anatomy and size. A potential solution may include catheter-based optical delivery as was demonstrated in intra-atrial imaging. Tissue perfusion is also accessible with myocardial contrast echography (MCE), which has been performed in patients. The PA alternative has the advantages of using endogenous contrast and conveys blood oxygenation.

PA imaging of intramyocardial stem cell injection treatment for cardiac repair following an MI (Berninger *et al* 2017) was explored by tracking fluorescently labelled stem cells in an animal model with multispectral

optoacoustic tomography (MSOT). Stem cell therapy for MI repair being currently debatable, positions PA imaging of stem cell treatment as a promising tool for researching, understanding and improving future treatments...

Of particular interest to cardiac interventions is the capability of non-invasively monitoring patients with elevated cardiovascular risk (Marcondes-Braga *et al* 2016b). The degree of myocardial necrosis can initially be detected through blood tests determining levels of biomarkers such as troponins or creatine phosphokinase (Mythili and Malathi 2015). Some of these byproducts are eliminated from the blood through the lungs in the exhaled air. In general, gas rebreathing techniques can measure and detect the presence of a multitude of biomarkers which may be related to specific diseases and/or indicate certain physiological imbalance (Navas *et al* 2012, Pereira *et al* 2015). Presence of acetone, pentene, nitric oxide, carbon monoxide, isoprene, pentane and ethane (byproducts of oxidative stress and subsequent lipid peroxidation), in the breath were shown to be related to heart failure (Weitz *et al* 1991, Cikach and Dweik 2012, Cheng *et al* 2014, Marcondes-Braga *et al* 2016a). Non-invasive PA breath gas analysis techniques are thus a viable option to evaluate heart failure development in MI (figure 9). For instance, ethylene, also shown to be related to oxidative stress, can be detected in the breath with PA gas rebreathing measurements. In fact, measures of expired ethylene using gas rebreathing measurement methods during coronary artery bypass grafting procedures and valvular surgery related well to organ reperfusion injury and to regional myocardial ischemia (Cristescu *et al* 2014). PA breath gas analysis can also measure cardiac output non-invasively, in real-time at rest and/or during exercise, to diagnose the severity of heart failure (Gabrielsen *et al* 2002, Agostoni *et al* 2005, Lang *et al* 2007). Monitoring cardiac output by the presence of specific biomarkers such as ethylene, ammonia or other products of lipid peroxidation were proven useful during surgery and at the bedside. Patented PA spectrometry based gas rebreathing technology has been successfully commercialized by a company named Innovision in Denmark. More specifically targeted PA gas analyser, such as ethylene sensors, can be bought from Sensor Sense in the Netherlands. Compared to traditional breath analysers based on mass spectrometry PA based spectrometers are more portable and less complex.

6. Directions for future instrumentation development

Development of a PA imaging system is a multimodal optimization problem defined by the application: light needs to reach and penetrate the targeted absorbing biological structure, while the US transducer needs to accommodate for the large bandwidth and low pressures of the PA signals, and all components need to be integrated into a realistic imaging system. Translation of PA imaging to any clinical application, including cardiovascular ones, depends critically on maturity of the technology. Being intrinsically multimodal, integration of robust, stable and safe devices that are suitable for regulatory approval is challenging. Optical delivery, acoustic functionality, data acquisition and the laser source need to be integrated into one system with validated performance and functionality.

To date, most research activity in the field has focused on intravascular imaging for the characterization of atherosclerosis and for intracardiac imaging of ablation lesions. These areas depend critically on invasive imaging tools, which means that the engineering challenge includes the economics of disposable devices. Nevertheless, the proof-of-concept studies, such as those discussed in this review, show that there is unique tissue contrast to be attained with PA imaging which may fulfil pressing clinical needs in the guidance of cardiovascular interventions, and that stable operation is possible.

Besides the challenges of multimodal systems and device engineering, a critical component of any PA imaging system is the light source. Historically, the field has developed on the ample availability of Q-switched solid-state lasers, which provide short pulses and high energies at a limited set of wavelengths, which usually are not the optimal ones for biomedical imaging. The popularity of solid-state lasers for PA imaging has furthered the development of sophisticated tuneable optical parametric oscillator systems (OPOs) pumped by Q-switched lasers. These deliver high-energy nanosecond pulses at any wavelength the biological system under study happens to require for optimal image contrast. Such lasers are versatile and powerful, but also expensive, noisy, fragile and with fluctuating optical pulse energy. They are scientific instruments, and not primarily suitable as components in a clinical imaging system that needs to be robust, portable, user-friendly, and economical. In addition, the PRF of many OPO systems tends to be on the low side for many applications. The first target for researchers interested in clinical translation of PA technology to a clinical setting is to identify an alternative to the tuneable laser that will deliver sufficient pulsed power at the right wavelengths.

A few inroads have been towards solving this problem. One approach has been to shift to a standard wavelength using an efficient stimulated Raman scattering medium to create a light source at the relevant frequency. The combination of the fundamental Nd:YAG wavelength and $Ba(NO_3)_2$ has been used for IVPA imaging at 1197 nm (Li *et al* 2013, Wang *et al* 2014). Many Raman active materials are available, and they may be coupled to a variety of base oscillators to access a range of biologically relevant wavelengths. Alternatively, diode lasers, pulsed or continuous wave (Stylogiannis *et al* 2018), may be part of the future solutions (Stylogiannis *et al* 2018,

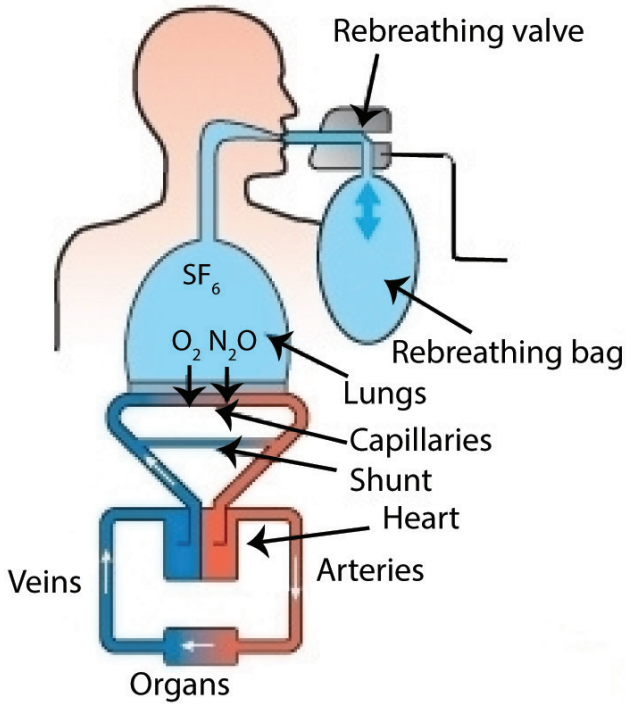

Figure 9. Gas rebreathing measurement principle. Concentrations of two inert gases, blood soluble and insoluble are measured to calculate cardiac output while taking into account lung volume among other correcting factors. Source: www.innovision.dk, with permission.

Upputuri and Pramanik 2018). There appears to be potentially usable contrast in imaging of atherosclerosis using these devices at standard wavelengths (Arabul 2018, Arabul *et al* 2017), and other wavelengths may become available in the future if there is sufficient demand. Light emitting diodes (LEDs) are also being explored for PA imaging, and may be a contender for some broad-illumination applications (Xia *et al* 2018, Zhu *et al* 2018). Compared to most PA lasers, LEDs are safer and allow for faster imaging frame rates, because they offer low-energy (nJ to μJ) pulses at high (several kHz) repetition rates.

For diode lasers as well as LEDs, generation of sufficiently energetic pulses with a duration that satisfies stress confinement is nontrivial. Efficient fiber coupling of these sources can be daunting. These considerations limit the utility of diodes for many of the applications discussed in this review. With suitably optimized optical delivery, these sources may find their way into handheld devices for applications such as described in figure 5. A review on the state of the art of photoacoustic imaging with laser diodes and LEDs can be found in Zhong *et al* (2018).

Another prominent engineering challenge that arises in many PA applications is the relative weakness of PA signals and the lack of control over their frequency content. As laser power can only be increased to the safety limit, and tends to be an expensive commodity, the solution must be found in sensitive detection. The ultrasound scanners and transducers that are used for PA signal detection have usually been optimized for pulse-echo imaging. Alternative transducer types such as capacitive and piezoelectric micromachined ultrasound transducers (CMUT, PMUT) and interferometric sensors are currently being investigated to accommodate for both the broadband nature of the PA signals generated and for the device integration/fabrication challenges (Nikoozadeh *et al* 2012, 2013, Ansari *et al* 2018, Mathews *et al* 2018). The power spectral density of PA signals tends to decrease with increasing frequency. Dedicated transducers with integrated amplification (Daeichin *et al* 2016a) or dedicated, high-impedance data acquisition hardware (Merčep *et al* 2015) aim to optimize the detection path for sensitivity. These technical hurdles must be scaled to ascertain informative, robust and affordable imaging in a clinical setting.

7. Summary

Cardiovascular interventions pose many imaging needs, which can potentially be tackled with PA imaging. Since the first applications in imaging blood vessels *ex vivo*, PA imaging has revealed a number of unique features in cardiovascular medicine that may be put to use in the guidance and monitoring of therapy. In atherosclerosis research, PA imaging can play a major role in determining the plaque features predicting vulnerability. This is based on the capability of relating macroscopic spectroscopic PA signals to microscopic features (Seeger *et al*

2016) in an experimental setup and capability of using these spectral features for *in vivo* identification of plaque composition.

Guidance of intracardiac ablation is another application where PA imaging can provide image contrast that is not available by any other means. Real-time monitoring of ablation lesions was reported using different methods, promising to unveil the progress of lesion formation to an otherwise blind cardiologist relying on model-based theory and experience. Evaluation of lesion gaps, discontinuity and in-depth electrical mapping could help the electrophysiology research field in understanding the patterns of atrial fibrillation and determining new methods to improve procedural success rates. We also discussed PA based gas rebreathing in the context of monitoring cardiac output, with an impact on MI assessment. For applications like direct infarct area sizing and detection of circulating thrombi, preclinical work has been done but the translational pathway is not yet clear.

This unique capability to visualize tissue contrast means that PA imaging has definitely a role in cardiovascular medicine research, and new applications are still emerging; especially with the on-going developments of more portable, safer, and faster laser sources. PA imaging is thus a promising, ionizing-radiation-free, contrast-agent-free solution for interventional imaging in cardiovascular interventions.

References

Abubakar I, Tillmann T and Banerjee A 2015 Global, regional, and national age-sex specific all-cause and cause-specific mortality for 240 causes of death, 1990–2013: a systematic analysis for the Global Burden of Disease Study 2013 *Lancet* **385** 117–71

Agostoni P, Cattadori G, Apostolo A, Contini M, Palermo P, Marenzi G and Wasserman K 2005 Noninvasive measurement of cardiac output during exercise by inert gas rebreathing technique: a new tool for heart failure evaluation *J. Am. Coll. Cardiol.* **46** 1779–81

Aguirre J, Schwarz M, Garzorz N, Omar M, Buehler A, Eyerich K and Ntziachristos V 2017 Precision assessment of label-free psoriasis biomarkers with ultra-broadband optoacoustic mesoscopy *Nat. Biomed. Eng.* **1** 0068

Ansari R, Zhang E Z, Desjardins A E and Beard P C 2018 All-optical forward-viewing photoacoustic probe for high-resolution 3D endoscopy *Light Sci. Appl.* **7** 75

Arabul M Ü 2018 Multi-wavelength photoacoustic imaging of the atherosclerotic carotid artery: a preclinical feasibility study *PhD Thesis* Technical University, Eindhoven

Arabul M U, Heres M, Rutten M C, van Sambeek M R, van de Vosse F N and Lopata R G 2017 Toward the detection of intraplaque hemorrhage in carotid artery lesions using photoacoustic imaging *J. Biomed. Opt.* **22** 41010

Aupperle H, Doll N, Walther T, Ullmann C, Schoon H-A and Wilhelm Mohr F 2005 Histological findings induced by different energy sources in experimental atrial ablation in sheep *Interact. Cardiovasc. Thorac. Surg.* **4** 450–5

Bai X, Gong X, Hau W, Lin R, Zheng J, Liu C, Zeng C, Zou X, Zheng H and Song L 2014 Intravascular optical-resolution photoacoustic tomography with a 1.1 mm diameter catheter *PLoS One* **9** e92463

Bajpai A, Savelieva I and Camm A J 2007 Epidemiology and economic burden of atrial fibrillation *US Cardiovasc Dis.* **1** 14–7

Beard P 2011 Biomedical photoacoustic imaging *Interface Focus* **1** 602–31

Beard P C and Mills T N 1997 Characterization of post mortem arterial tissue using time-resolved photoacoustic spectroscopy at 436, 461 and 532 nm *Phys. Med. Biol.* **42** 177–98

Berninger M T *et al* 2017 Detection of intramyocardially injected DiR-labeled mesenchymal stem cells by optical and optoacoustic tomography *Photoacoustics* **6** 37–47

Bouchard R, Dana N, Di Biase L, Natale A and Emelianov S 2012 Photoacoustic characterization of radiofrequency ablation lesions *Proc. SPIE* **8223** 82233K

Brochu F M, Brunker J, Joseph J, Tomaszewski M R, Morscher S and Bohndiek S E 2017 Towards quantitative evaluation of tissue absorption coefficients using light fluence correction in optoacoustic tomography *IEEE Trans. Med. Imaging* **36** 322–31

Bui N Q, Hlaing K K, Lee Y W, Kang H W and Oh J 2017 *Ex vivo* detection of macrophages in atherosclerotic plaques using intravascular ultrasonic-photoacoustic imaging *Phys. Med. Biol.* **62** 501–16

Cao Y, Hui J, Kole A, Wang P, Yu Q, Chen W, Sturek M and Cheng J X 2016 High-sensitivity intravascular photoacoustic imaging of lipid-laden plaque with a collinear catheter design *Sci. Rep.* **6** 25236

Cao Y, Kole A, Hui J, Zhang Y, Mai J, Alloosh M, Sturek M and Cheng J X 2018 Fast assessment of lipid content in arteries *in vivo* by intravascular photoacoustic tomography *Sci. Rep.* **8** 2400

Cheng S *et al* 2014 Association of exhaled carbon monoxide with subclinical cardiovascular disease and their conjoint impact on the incidence of cardiovascular outcomes *Eur. Heart J.* **35** 2980–7

Chugh S S *et al* 2014 Worldwide epidemiology of atrial fibrillation a global burden of disease 2010 study *Circulation* **129** 837–47

Cikach F S Jr and Dweik R A 2012 Cardiovascular biomarkers in exhaled breath *Prog. Cardiovasc. Dis.* **55** 34–43

Cohen G I, Aboufakher R, Bess R, Frank J, Othman M, Doan D, Mesiha N, Rosman H S and Szpunar S 2013 Relationship between carotid disease on ultrasound and coronary disease on CT angiography *JACC Cardiovasc. Imaging* **6** 1160–7

Craven T E, Ryu J E, Espeland M A, Kahl F R, Mckinney W M, Toole J F, Mcmahan M R, Thompson C J, Heiss G and Crouse J R 1990 Evaluation of the associations between carotid-artery atherosclerosis and coronary-artery stenosis—a case-control study *Circulation* **82** 1230–42

Cristescu S M, Kiss R, te Lintel Hekkert S, Dalby M, Harren F J, Risby T H and Marczin N 2014 Real-time monitoring of endogenous lipid peroxidation by exhaled ethylene in patients undergoing cardiac surgery *Am. J. Physiol. Lung Cell. Mol. Physiol.* **307** L509–15

Daeichin V, Wu M, De Jong N, van der Steen A F and van Soest G 2016b Frequency analysis of the photoacoustic signal generated by coronary atherosclerotic plaque *Ultrasound Med. Biol.* **42** 2017–25

Daeichin V *et al* 2016a A broadband polyvinylidene difluoride-based hydrophone with integrated readout circuit for intravascular photoacoustic imaging *Ultrasound Med. Biol.* **42** 1239–43

Dana N, Di Biase L, Natale A, Emelianov S and Bouchard R 2014 *In vitro* photoacoustic visualization of myocardial ablation lesions *Heart Rhythm* **11** 150–7

Dana N, Fowler R A, Allen A, Zoldan J, Suggs L and Emelianov S 2016 *In vitro* photoacoustic sensing of calcium dynamics with arsenazo III *Laser Phys. Lett.* **13** 075603

de Groot N *et al* 2016 Direct proof of endo-epicardial asynchrony of the atrial wall during atrial fibrillation in humans *Circ. Arrhythm. Electrophysiol.* **9** e003648
Diebold G J, Sun T and Khan M I 1991 Photoacoustic monopole radiation in 1-dimension, 2-dimension, and 3-dimension *Phys. Rev. Lett.* **67** 3384–7
Dima A, Burton N C and Ntziachristos V 2014 Multispectral optoacoustic tomography at 64, 128, and 256 channels *J. Biomed. Opt.* **19** 36021
Dima A and Ntziachristos V 2012 Non-invasive carotid imaging using optoacoustic tomography *Opt. Express* **20** 25044–57
Dukkipati S R *et al* 2013 Pulmonary vein isolation using a visually guided laser balloon catheter: the first 200-patient multicenter clinical experience *Circulation* **6** 467–72
Emelianov S, Wang B, Su J, Karpiouk A, Yantsen E, Sokolov K, Amirian J, Smalling R and Sethuraman S 2008 Intravascular ultrasound and photoacoustic imaging *Conf. Proc. IEEE Engineering in Medicine and Biology Society* pp 2–5
Falk E, Nakano M, Bentzon J F, Finn A V and Virmani R 2013 Update on acute coronary syndromes: the pathologists' view *Eur. Heart J.* **34** 719–28
Gabrielsen A, Videbaek R, Schou M, Damgaard M, Kastrup J and Norsk P 2002 Non-invasive measurement of cardiac output in heart failure patients using a new foreign gas rebreathing technique *Clin. Sci.* **102** 247–52
Galanzha E I, Sarimollaoglu M, Nedosekin D A, Keyrouz S G, Mehta J L and Zharov V P 2011 *In vivo* flow cytometry of circulating clots using negative photothermal and photoacoustic contrasts *Cytometry* A **79** 814–24
Galanzha E I, Viegas M G, Malinsky T I, Melerzanov A V, Juratli M A, Sarimollaoglu M, Nedosekin D A and Zharov V P 2016 *In vivo* acoustic and photoacoustic focusing of circulating cells *Sci. Rep.* **6** 21531
Galanzha E I and Zharov V P 2011 *In vivo* photoacoustic and photothermal cytometry for monitoring multiple blood rheology parameters *Cytometry* A **79** 746–57
Galanzha E I and Zharov V P 2012 Photoacoustic flow cytometry *Methods* **57** 280–96
Gandjbakhche A H, Bonner R F, Arai A E and Balaban R S 1999 Visible-light photon migration through myocardium *in vivo Am. J. Physiol.* **277** H698–704
Ganjehei L, Razavi M and Rasekh A 2011 Catheter-based ablation of atrial fibrillation: a brief overview *Tex Heart Inst. J.* **38** 361–3
Glatz J, Deliolanis N C, Buehler A, Razansky D and Ntziachristos V 2011 Blind source unmixing in multi-spectral optoacoustic tomography *Opt. Express* **19** 3175–84
Herken U, Silver A, Kaufman C and Freeman G A 2016 *Transesophageal or Transtracheal Cardiac Monitoring by Optical Spectroscopy* ed USPTO ZOLL Medical Corp *Patent* US Patent Application No. 14/927,104
Holman R T and Edmondson P R 1956 Near-infrared spectra of fatty acids and some related substances *Anal. Chem.* **28** 1533–8
Hong S J *et al* 2015 Effect of intravascular ultrasound-guided versus angiography-guided everolimus-eluting stent implantation: the IVUS-XPL randomized clinical trial *JAMA* **314** 2155–63
Hu S, Maslov K and Wang L V 2009 Noninvasive label-free imaging of microhemodynamics by optical-resolution photoacoustic microscopy *Opt. Express* **17** 7688–93
Hu S and Wang L V 2010 Photoacoustic imaging and characterization of the microvasculature *J. Biomed. Opt.* **15** 011101
Iskander-Rizk S, Kruizinga P, van der Steen A F W and van Soest G 2018a Spectroscopic photoacoustic imaging of radiofrequency ablation in the left atrium *Biomed. Opt. Express* **9** 1309–22
Iskander-Rizk S, Springeling G, Kruizinga P, Beurskens R H S H, Van der Steen A F W and Van Soest G 2018b Photoacoustic-enabled RF ablation catheters for lesion monitoring *IEEE Int. Ultrasonics Symp.* pp 1–4
Iskander-Rizk S, Wu M, Springeling G, Mastik F, Beurskens R H S H, van der Steen A F W and van Soest G 2018c Catheter design optimization for practical intravascular photoacoustic imaging (IVPA) of vulnerable plaques *Proc. SPIE* **10471** 1047111
Isner J M, Pickering J G and Mosseri M 1992 Laser-induced dissections: pathogenesis and implications for therapy *J. Am. Coll. Cardiol.* **19** 1619–21
Ivankovic I, Merčep E, Schmedt C-G, Deán-Ben X L and Razansky D 2019 Real-time volumetric assessment of the human carotid artery: handheld multispectral optoacoustic tomography *Radiology* **291** 45–50
Jang J-S *et al* 2014 Intravascular ultrasound-guided implantation of drug-eluting stents to improve outcome: a meta-analysis *JACC Cardiovasc. Interv.* **7** 233–43
Jansen K, van der Steen A F, van Beusekom H M, Oosterhuis J W and van Soest G 2011 Intravascular photoacoustic imaging of human coronary atherosclerosis *Opt. Lett.* **36** 597–9
Jansen K, van der Steen A F, Wu M, van Beusekom H M, Springeling G, Li X, Zhou Q, Shung K K, de Kleijn D P and van Soest G 2014a Spectroscopic intravascular photoacoustic imaging of lipids in atherosclerosis *J. Biomed. Opt.* **19** 026006
Jansen K, van Soest G and van der Steen A F W 2014b Intravascular photoacoustic imaging: a new tool for vulnerable plaque identification *Ultrasound Med. Biol.* **40** 1037–48
Jansen K, Wu M, van der Steen A F and van Soest G 2013 Lipid detection in atherosclerotic human coronaries by spectroscopic intravascular photoacoustic imaging *Opt. Express* **21** 21472–84
Jansen K, Wu M, van der Steen A F and van Soest G 2014c Photoacoustic imaging of human coronary atherosclerosis in two spectral bands *Photoacoustics* **2** 12–20
Ji X, Xiong K, Yang S and Xing D 2015 Intravascular confocal photoacoustic endoscope with dual-element ultrasonic transducer *Opt. Express* **23** 9130–6
Juratli M A, Menyaev Y A, Sarimollaoglu M, Melerzanov A V, Nedosekin D A, Culp W C, Suen J Y, Galanzha E I and Znarov V P 2018 Noninvasive label-free detection of circulating white and red blood clots in deep vessels with a focused photoacoustic probe *Biomed. Opt. Express* **9** 5667–77
Juratli M A, Menyaev Y A, Sarimollaoglu M, Siegel E R, Nedosekin D A, Suen J Y, Melerzanov A V, Juratli T A, Galanzha E I and Zharov V P 2016 Real-time label-free embolus detection using *in vivo* photoacoustic flow cytometry *PLoS One* **11** e0156269
Karpiouk A B, Wang B, Amirian J, Smalling R W and Emelianov S Y 2012 Feasibility of *in vivo* intravascular photoacoustic imaging using integrated ultrasound and photoacoustic imaging catheter *J. Biomed. Opt.* **17** 96008–1
Kole A, Cao Y, Hui J, Bolad I A, Alloosh M, Cheng J-X and Sturek M 2018 Comparative quantification of arterial lipid by intravascular photoacoustic-ultrasound imaging and near-infrared spectroscopy-intravascular ultrasound *J. Cardiovasc. Transl. Res.* **12** 211–20
Kruizinga P, van der Steen A F, de Jong N, Springeling G, Robertus J L, van der Lugt A and van Soest G 2014 Photoacoustic imaging of carotid artery atherosclerosis *J. Biomed. Opt.* **19** 110504
Landa F J O, Dean-Ben X L, Sroka R and Razansky D 2017 Volumetric optoacoustic temperature mapping in photothermal therapy *Sci. Rep.* **7** 9695
Lang C C, Karlin P, Haythe J, Tsao L and Mancini D M 2007 Ease of noninvasive measurement of cardiac output coupled with peak VO_2 determination at rest and during exercise in patients with heart failure *Am. J. Cardiol.* **99** 404–5
Li L and Tearney G J 2017 *Apparatus, Systems and Methods for Characterizing, Imaging and/or Modifying an Object* (General Hospital Corp) *Patent* US Patent Application No. 15/115,348

Li R, Slipchenko M N, Wang P and Cheng J-X 2013 Compact high power barium nitrite crystal-based Raman laser at 1197 nm for photoacoustic imaging of fat *J. Biomed. Opt.* **18** 040502
Li X, Wei W, Zhou Q, Shung K K and Chen Z 2012 Intravascular photoacoustic imaging at 35 and 80 MHz *J. Biomed. Opt.* **17** 106005
Li Y and Chen Z P 2018 Multimodal intravascular photoacoustic and ultrasound imaging *Biomed. Eng. Lett.* **8** 193–201
Li Z, Chen H, Zhou F, Li H and Chen W R 2015 Interstitial photoacoustic sensor for the measurement of tissue temperature during interstitial laser phototherapy *Sensors* **15** 5583–93
Lin H A, Dean-Ben X L, Ivankovic I, Kimm M A, Kosanke K, Haas H, Meier R, Lohofer F, Wildgruber M and Razansky D 2017 Characterization of cardiac dynamics in an acute myocardial infarction model by four-dimensional optoacoustic and magnetic resonance imaging *Theranostics* **7** 4470–9
Luke G P and Emelianov S Y 2014 Optimization of *in vivo* spectroscopic photoacoustic imaging by smart optical wavelength selection *Opt. Lett.* **39** 2214–7
Lv J, Peng Y, Li S, Guo Z, Zhao Q, Zhang X and Nie L 2018 Hemispherical photoacoustic imaging of myocardial infarction: *in vivo* detection and monitoring *Eur. Radiol.* **28** 2176–83
Manohar S and Razansky D 2016 Photoacoustics: a historical review *Adv. Opt. Photonics* **8** 586–617
Marcondes-Braga F G, Batista G L, Bacal F and Gutz I 2016a Exhaled breath analysis in heart failure *Curr. Heart Fail. Rep.* **13** 166–71
Marcondes-Braga F G *et al* 2016b Impact of exhaled breath acetone in the prognosis of patients with heart failure with reduced ejection fraction (HFrEF). One year of clinical follow-up *PLoS One* **11** e0168790
Mathews S J, Little C, Loder C D, Rakhit R D, Xia W F, Zhang E Z, Beard P C, Finlay M C and Desjardins A E 2018 All-optical dual photoacoustic and optical coherence tomography intravascular probe *Photoacoustics* **11** 65–70
Mercep E, Dean-Ben X L and Razansky D 2018 Imaging of blood flow and oxygen state with a multi-segment optoacoustic ultrasound array *Photoacoustics* **10** 48–53
Merčep E, Jeng G, Morscher S, Pai-Chi L and Razansky D 2015 Hybrid optoacoustic tomography and pulse-echo ultrasonography using concave arrays *IEEE Trans. Ultrason. Ferroelectr. Freq. Control* **62** 1651–61
Mintz G S and Guagliumi G 2017 Intravascular imaging in coronary artery disease *Lancet* **390** 793–809
Mukaddim R A, Rodgers A, Hacker T A, Heinmiller A and Varghese T 2018 Real-time *in vivo* photoacoustic imaging in the assessment of myocardial dynamics in murine model of myocardial ischemia *Ultrasound Med. Biol.* **44** 2155–64
Myat A, Gershlick A H and Gershlick T 2012 *Landmark Papers in Cardiovascular Medicine* (Oxford: Oxford University Press)
Mythili S and Malathi N 2015 Diagnostic markers of acute myocardial infarction *Biomed. Rep.* **3** 743–8
Navas M J, Jimenez A M and Asuero A G 2012 Human biomarkers in breath by photoacoustic spectroscopy *Clin. Chim Acta* **413** 1171–8
Nikoozadeh A, Chang C L, Choe J W, Bhuyan A, Lee B C, Moini A and Khuri-Yakub P T 2013 An integrated ring CMUT array for endoscopic ultrasound and photoacoustic imaging *IEEE Int. Ultrasonics Symp.* pp 1170–3
Nikoozadeh A, Choe J W, Kothapalli S R, Moini A, Sanjani S S, Kamaya A, Oralkan O, Gambhir S S and Khuri-Yakub P T 2012 Photoacoustic imaging using a ^{9}F microlinear CMUT ICE catheter *IEEE Int. Ultrasonics Symp.* pp 24–7
Ouyang F *et al* 2005 Recovered pulmonary vein conduction as a dominant factor for recurrent atrial tachyarrhythmias after complete circular isolation of the pulmonary veins: lessons from double Lasso technique *Circulation* **111** 127–35
Pang G A, Bay E, Dean-Ben X L and Razansky D 2015 Three-dimensional optoacoustic monitoring of lesion formation in real time during radiofrequency catheter ablation *J. Cardiovasc. Electrophysiol.* **26** 339–45
Pereira J, Porto-Figueira P, Cavaco C, Taunk K, Rapole S, Dhakne R, Nagarajaram H and Camara J S 2015 Breath analysis as a potential and non-invasive frontier in disease diagnosis: an overview *Metabolites* **5** 3–55
Qin H, Zhao Y, Zhang J, Pan X, Yang S and Xing D 2016 Inflammation-targeted gold nanorods for intravascular photoacoustic imaging detection of matrix metalloproteinase-2 (MMP2) in atherosclerotic plaques *Nanomedicine* **12** 1765–74
Qin H, Zhou T, Yang S, Chen Q and Xing D 2013 Gadolinium(III)-gold nanorods for MRI and photoacoustic imaging dual-modality detection of macrophages in atherosclerotic inflammation *Nanomedicine* **8** 1611–24
Quan K J and Hodgson J M 1996 Comparison of tissue disruption caused by excimer and midinfrared lasers in clinical simulation *Cathet. Cardiovasc. Diagn.* **38** 50–5
Rao B, Zhang R, Li L, Shao J Y and Wang L V 2017 Photoacoustic imaging of voltage responses beyond the optical diffusion limit *Sci. Rep.* **7** 2560
Razansky D, Harlaar N J, Hillebrands J L, Taruttis A, Herzog E, Zeebregts C J, van Dam G M and Ntziachristos V 2012 Multispectral optoacoustic tomography of matrix metalloproteinase activity in vulnerable human carotid plaques *Mol. Imaging Biol.* **14** 277–85
Razansky D, Vinegoni C and Ntziachristos V 2007 Multispectral photoacoustic imaging of fluorochromes in small animals *Opt. Lett.* **32** 2891–3
Rebling J, Oyaga Landa F J, Dean-Ben X L, Douplik A and Razansky D 2018 Integrated catheter for simultaneous radio frequency ablation and optoacoustic monitoring of lesion progression *Opt. Lett.* **43** 1886–9
Reddy K, Khaliq A and Henning R J 2015 Recent advances in the diagnosis and treatment of acute myocardial infarction *World J. Cardiol.* **7** 243–76
Ricles L M, Nam S Y, Trevino E A, Emelianov S Y and Suggs L J 2014 A dual gold nanoparticle system for mesenchymal stem cell tracking *J. Mater. Chem.* B **2** 8220–30
Ridker P M *et al* 2017 Antiinflammatory therapy with canakinumab for atherosclerotic disease *New Engl. J. Med.* **377** 1119–31
Roes S D *et al* 2009 Infarct tissue heterogeneity assessed with contrast-enhanced MRI predicts spontaneous ventricular arrhythmia in patients with ischemic cardiomyopathy and implantable cardioverter-defibrillator *Circ. Cardiovasc. Imaging* **2** 183
Schaar J A, de Korte C L, Mastik F, Baldewsing R, Regar E, de Feyter P, Slager C J, van der Steen A F W and Serruys P W 2003 Intravascular palpography for high-risk vulnerable plaque assessment *Herz* **28** 488–95
Schaar J A *et al* 2004 Terminology for high-risk and vulnerable coronary artery plaques *Eur. Heart J.* **25** 1077–82
Schmitt C, Deisenhofer I and Zrenner B 2006 *Catheter Ablation of Cardiac Arrhythmias: a Practical Approach* (Berlin: Springer)
Seeger M, Karlas A, Soliman D, Pelisek J and Ntziachristos V 2016 Multimodal optoacoustic and multiphoton microscopy of human carotid atheroma *Photoacoustics* **4** 102–11
Sethuraman S, Amirian J H, Litovsky S H, Smalling R W and Emelianov S Y 2008 Spectroscopic intravascular photoacoustic imaging to differentiate atherosclerotic plaques *Opt. Express* **16** 3362–7
Sethuraman S, Amirian J H, Litovsky S H, Smalling R W and Emelianov S Y 2007 *Ex vivo* characterization of atherosclerosis using intravascular photoacoustic imaging *Opt. Express* **15** 16657–66
Silvestre-Roig C, de Winther M P, Weber C, Daemen M J, Lutgens E and Soehnlein O 2014 Atherosclerotic plaque destabilization mechanisms, models, and therapeutic strategies *Circ. Res.* **114** 214–26
Singh-Moon R P, Marboe C C and Hendon C P 2015 Near-infrared spectroscopy integrated catheter for characterization of myocardial tissues: preliminary demonstrations to radiofrequency ablation therapy for atrial fibrillation *Biomed. Opt. Express* **6** 2494–511

Sowers T and Emelianov S 2018 Exogenous imaging contrast and therapeutic agents for intravascular photoacoustic imaging and image-guided therapy *Phys. Med. Biol.* **63**

Sowers T, VanderLaan D, Karpiouk A, Donnelly E M, Smith E and Emelianov S 2018 Laser threshold and cell damage mechanism for intravascular photoacoustic imaging *Lasers Surg. Med.* **51** 466–74

Srivatsa U N, Danielsen B, Amsterdam E A, Pezeshkian N, Yang Y, Nordsieck E, Fan D, Chiamvimonvat N and White R H 2018 CAABL-AF (California study of ablation for atrial fibrillation): mortality and stroke, 2005 to 2013 *Circulation* **11** e005739

Steinbeck G, Sinner M F, Lutz M, Muller-Nurasyid M, Kaab S and Reinecke H 2018 Incidence of complications related to catheter ablation of atrial fibrillation and atrial flutter: a nationwide in-hospital analysis of administrative data for Germany in 2014 *Eur. Heart J.* **39** 4020–9

Stylogiannis A, Prade L, Buehler A, Aguirre J, Sergiadis G and Ntziachristos V 2018 Continuous wave laser diodes enable fast optoacoustic imaging *Photoacoustics* **9** 31–8

Topaz O, McIvor M, Stone G W, Krucoff M W, Perin E C, Foschi A E, Sutton J, Nair R and deMarchena E 1998 Acute results, complications, and effect of lesion characteristics on outcome with the solid-state, pulsed-wave, mid-infrared laser angioplasty system: final multicenter registry report. Holmium:YAG laser multicenter investigators *Lasers Surg. Med.* **22** 228–39

Topaz O, Minisi A J, Morris C, Mohanty P K and Carr M E 1996 Photoacoustic fibrinolysis: pulsed-wave, mid-infrared laser-clot interaction *J. Thromb. Thrombolysis* **3** 209–14

Tuchin V V, Tarnok A and Zharov V P 2011 *In vivo* flow cytometry: a horizon of opportunities *Cytometry* A **79** 737–45

Upputuri P K and Pramanik M 2018 Fast photoacoustic imaging systems using pulsed laser diodes: a review *Biomed. Eng. Lett.* **8** 167–81

van den Berg P J, Daoudi K and Steenbergen W 2015 Review of photoacoustic flow imaging: its current state and its promises *Photoacoustics* **3** 89–99

van Leeuwen T G, Meertens J H, Velema E, Post M J and Borst C 1993 Intraluminal vapor bubble induced by excimer laser pulse causes microsecond arterial dilation and invagination leading to extensive wall damage in the rabbit *Circulation* **87** 1258–63

van Leeuwen T G, van Erven L, Meertens J H, Motamedi M, Post M J and Borst C 1992 Origin of arterial wall dissections induced by pulsed excimer and mid-infrared laser ablation in the pig *J. Am. Coll. Cardiol.* **19** 1610–8

van Soest G, Marcu L, Bouma B E and Regar E 2017 Intravascular imaging for characterization of coronary atherosclerosis *Curr. Opin. Biomed. Eng.* **3** 1–12

VanderLaan D, Karpiouk A B, Yeager D and Emelianov S 2017 Real-time intravascular ultrasound and photoacoustic imaging *IEEE Trans. Ultrason. Ferroelectr. Freq. Control* **64** 141–9

Virmani R, Burke A P, Farb A and Kolodgie F D 2006 Pathology of the vulnerable plaque *J. Am. Coll. Cardiol.* **47** C13–8

Virmani R, Kolodgie F D, Burke A P, Farb A and Schwartz S M 2000 Lessons from sudden coronary death—a comprehensive morphological classification scheme for atherosclerotic lesions *Arterioscler. Thromb. Vasc. Biol.* **20** 1262–75

Wang B, Karpiouk A, Yeager D, Amirian J, Litovsky S, Smalling R and Emelianov S 2012a *In vivo* intravascular ultrasound-guided photoacoustic imaging of lipid in plaques using an animal model of atherosclerosis *Ultrasound Med. Biol.* **38** 2098–103

Wang B, Karpiouk A, Yeager D, Amirian J, Litovsky S, Smalling R and Emelianov S 2012b Intravascular photoacoustic imaging of lipid in atherosclerotic plaques in the presence of luminal blood *Opt. Lett.* **37** 1244–6

Wang B, Su J L, Amirian J, Litovsky S H, Smalling R and Emelianov S 2010 Detection of lipid in atherosclerotic vessels using ultrasound-guided spectroscopic intravascular photoacoustic imaging *Opt. Express* **18** 4889–97

Wang B, Yantsen E, Larson T, Karpiouk A B, Sethuraman S, Su J L, Sokolov K and Emelianov S Y 2009 Plasmonic intravascular photoacoustic imaging for detection of macrophages in atherosclerotic plaques *Nano Lett.* **9** 2212–7

Wang L V 2009 *Photoacoustic Imaging and Spectroscopy* (Boca Raton, FL: CRC Press)

Wang P *et al* 2014 High-speed intravascular photoacoustic imaging of lipid-laden atherosclerotic plaque enabled by a 2 kHz barium nitrite Raman laser *Sci. Rep.* **4** 6889

Wang P, Wang H W, Sturek M and Cheng J X 2012c Bond-selective imaging of deep tissue through the optical window between 1600 and 1850 nm *J. Biophotonics* **5** 25–32

Weitz Z W, Birnbaum A J, Sobotka P A, Zarling E J and Skosey J L 1991 High breath pentane concentrations during acute myocardial-infarction *Lancet* **337** 933–5

WHO 2015 Cardiovascular diseases fact sheet (https://www.who.int/health-topics/cardiovascular-diseases/)

Williamson W A, Aretz H T, Weng G, Shahian D M, Hamilton W M, Pankratov M M and Shapshay S M 1993 *In vitro* decalcification of aortic valve leaflets with the Er:YSGG laser, Ho:YAG laser, and the Cavitron ultrasound surgical aspirator *Lasers Surg. Med.* **13** 421–8

Wolf P A, Dawber T R, Thomas H E J and Kannel W B 1978 Epidemiologic assessment of chronic atrial fibrillation and risk of stroke: the Framingham study *Neurology* **28** 973–7

Wright M 2015 Real-time atrial wall imaging *Heart Rhythm* **12** 1836–7

Wu M, Jansen K, Springeling G, van der Steen A F and van Soest G 2014 Impact of device geometry on the imaging characteristics of an intravascular photoacoustic catheter *Appl. Opt.* **53** 8131–9

Wu M, Jansen K, van der Steen A F and van Soest G 2015 Specific imaging of atherosclerotic plaque lipids with two-wavelength intravascular photoacoustics *Biomed. Opt. Express* **6** 3276–86

Wu M, Springeling G, Lovrak M, Mastik F, Iskander-Rizk S, Wang T S, van Beusekom H M M, van der Steen A F W and Van Soest G 2017 Real-time volumetric lipid imaging *in vivo* by intravascular photoacoustics at 20 frames per second *Biomed. Opt. Express* **8** 943–53

Wu X, Sanders J L, Zhang X, Yamaner F Y and Oralkan O 2019 An FPGA-based backend system for intravascular photoacoustic and ultrasound imaging *IEEE Trans. Ultrason. Ferroelectr. Freq. Control* **66** 45–56

Xia W, Singh M K A, Maneas E, Sato N, Shigeta Y, Agano T, Ourselin S, West S J and Desjardins A E 2018 Handheld real-time LED-based photoacoustic and ultrasound imaging system for accurate visualization of clinical metal needles and superficial vasculature to guide minimally invasive procedures *Sensors* **18** 1394

Zemp R J 2010 Quantitative photoacoustic tomography with multiple optical sources *Appl. Opt.* **49** 3566–72

Zemp R J, Song L, Bitton R, Shung K K and Wang L V 2008 Realtime photoacoustic microscopy of murine cardiovascular dynamics *Opt. Express* **16** 18551–6

Zhang H K *et al* 2017 Listening to membrane potential: photoacoustic voltage-sensitive dye recording *J. Biomed. Opt.* **22** 045006

Zhang J *et al* 2018 Intravascular ultrasound-versus angiography-guided drug-eluting stent implantation: the ULTIMATE trial *J. Am. Coll. Cardiol.* **72** 3126–37

Zhang J, Yang S, Ji X, Zhou Q and Xing D 2014 Characterization of lipid-rich aortic plaques by intravascular photoacoustic tomography: *ex vivo* and *in vivo* validation in a rabbit atherosclerosis model with histologic correlation *J. Am. Coll. Cardiol.* **64** 385–90

Zhong H T, Duan T Y, Lan H R, Zhou M and Gao F 2018 Review of low-cost photoacoustic sensing and imaging based on laser diode and light-emitting diode *Sensors* **18** 2264

Zhu Y, Xu G, Yuan J, Jo J, Gandikota G, Demirci H, Agano T, Sato N, Shigeta Y and Wang X 2018 Light emitting diodes based photoacoustic imaging and potential clinical applications *Sci. Rep.* **8** 9885